

---

**Pacific Northwest  
National Laboratory**

Operated by Battelle for the  
U.S. Department of Energy

# Characterization of Suspect Fuel Rod Pieces from the 105 K West Basin

C. H. Delegard  
A. J. Schmidt  
K. N. Pool  
B. M. Thornton

September 2006



Prepared for the U.S. Department of Energy  
under Contract DE-AC05-76RL01830

---

## DISCLAIMER

This report was prepared as an account of work sponsored by an agency of the United States Government. Neither the United States Government nor any agency thereof, nor Battelle Memorial Institute, nor any of their employees, makes **any warranty, express or implied, or assumes any legal liability or responsibility for the accuracy, completeness, or usefulness of any information, apparatus, product, or process disclosed, or represents that its use would not infringe privately owned rights.** Reference herein to any specific commercial product, process, or service by trade name, trademark, manufacturer, or otherwise does not necessarily constitute or imply its endorsement, recommendation, or favoring by the United States Government or any agency thereof, or Battelle Memorial Institute. The views and opinions of authors expressed herein do not necessarily state or reflect those of the United States Government or any agency thereof.

PACIFIC NORTHWEST NATIONAL LABORATORY  
*operated by*  
BATTELLE  
*for the*  
UNITED STATES DEPARTMENT OF ENERGY  
*under Contract DE-AC05-76RL01830*

**Printed in the United States of America**

**Available to DOE and DOE contractors from the  
Office of Scientific and Technical Information,  
P.O. Box 62, Oak Ridge, TN 37831-0062;  
ph: (865) 576-8401  
fax: (865) 576-5728  
email: reports@adonis.osti.gov**

**Available to the public from the National Technical Information Service,  
U.S. Department of Commerce, 5285 Port Royal Rd., Springfield, VA 22161  
ph: (800) 553-6847  
fax: (703) 605-6900  
email: orders@ntis.fedworld.gov  
online ordering: <http://www.ntis.gov/ordering.htm>**



This document was printed on recycled paper.

(9/2003)

# Characterization of Suspect Fuel Rod Pieces from the 105 K West Basin

C. H. Delegard  
A. J. Schmidt  
K. N. Pool  
B. M. Thornton

September 2006

Prepared for the U.S. Department of Energy  
under Contract DE-AC05-76RL01830

Pacific Northwest National Laboratory  
Richland, Washington 99352

This report was originally published in July 2006. In September 2006, minor transcription errors were discovered in the plutonium isotopic mass-percent values reported in Table 3.5 for the suspect fuel sample SF-4-2. This report has, therefore, been updated to correct these minor inconsistencies. The original values were those for a single analysis of sample SF-4-2; the correct values are averages of the three analytical results obtained for SF-4-2. Example calculations given on pages 3.12 and 3.13 also were based on incorrect values.

This revision of the report corrects the plutonium isotopic values in Table 3.5 and presents the example calculations given on page 3.13 using the corrected plutonium mass% values. The example equation on page 3.12 was modified to provide the atom-percent values for natural uranium (instead of those of SF-4-2) to show that 0.7200 atom%  $^{235}\text{U}$  in natural uranium is 0.711 mass%  $^{235}\text{U}$ . Three other transcription errors, which varied from the true values by 1 in the least significant figure for  $^{239}\text{Pu}$  in sample SF-8-1 in Table S.1 and for  $^{238}\text{Pu}$ , AEA, in sample SF-4-2 and for  $^{238}\text{Pu}$  in sample SF-12-3 in Table 3.4, also were corrected. Also, minor modifications to Table A.1 were made to improve clarity.

The transcription errors corrected in this revised report were limited to the identified tables and text. The data provided in the Data Package supporting this report were not affected and therefore the Data Package has not been revised.

## Summary

This report provides physical and radiochemical characterization results from examinations and laboratory analyses performed on ~0.5 to 0.6-inch diameter rod pieces found in the 105 K West (KW) Basin that were suspected to be from nuclear reactor fuel. The characterization results will be used to establish the technical basis for adding this material to the contents of one of the final Multi-Canister Overpacks (MCOs) that will be loaded out of the KW Basin in FY2007 at a time depending on project priorities. The receipt and examinations of the suspect rod pieces were performed consistent with the requirements of the Fluor Hanford/K Basin Closure (FH/KBC) Sampling and Analysis Plan (SAP), KBC-29054 (Baker et al. 2006).

Fifteen fuel rod pieces were found during the clean out of the KW Basin. Based on lack of specific credentials, documentation, or obvious serial numbers, none of the items could be positively identified nor could their sources or compositions be described. Item weights and dimensions measured in the KW Basin indicated densities consistent with the suspect fuel rods containing uranium dioxide (UO<sub>2</sub>), uranium metal, or being empty. Measurements performed in the KW Basin showed that the items having solid contents have radioactivity levels above background. Extensive review of the Hanford Site technical literature led to the postulation that these pieces likely were irradiated test fuel prepared to support the development of the Hanford "New Production Reactor," later called N Reactor.

To obtain definitive data on the composition of the suspect fuel, 4 representative fuel rod pieces, 9- to 13.5-inches long, were selected from the 15 rod piece population. [In the 325 Building, the suspect fuel rod pieces were given the designations of SF-4, SF-5, SF-8 and SF-12, which correspond to SAP designations for rod pieces, #4, #5, #8, and #12, respectively.] All four had densities corresponding to oxide fuel. The 4 items were shipped from the KW Basin to the Pacific Northwest National Laboratory (PNNL) Radiological Processing Laboratory (RPL; also known as the 325 Building). A PAS-1 cask and shielded sample container (SSC) were used to ship the selected rod pieces. At the RPL, the suspect fuel rods were removed from the PAS-1 cask, placed in the hot cell, their identities confirmed, visually examined, and physically characterized. The characterization confirmed the outer diameter of each item to be about 0.55-inch with a cladding wall thickness of about 0.031 inch. The black to dark grey fuel material appeared to totally fill the cladding inner diameter and have open interconnected porosity. The appearance was consistent with uranium oxide based fuels and the apparent fuel density confirmed values derived from KW Basin evaluations.

Following physical evaluation, KBC and PNNL staff developed cutting diagrams based on SAP requirements and general observations of the rod pieces. Three of the 4 fuel rods (SF-4, SF-8, and SF-12) were sectioned by transverse cutting with a diamond saw. Two ~1/8-inch thick disks samples were cut from each of the 3 fuel rods. One disk sample was taken from each rod near the center (samples SF-4-1, SF-8-1, and SF-12-3) and one sample from each rod was taken ~2 inches from an end (samples SF-4-2, SF-8-2, and SF-12-2). The fourth fuel rod piece (SF-5) was stored as a contingent for later examination in case questions developed from results obtained from the three sectioned fuel rods. No need for examining SF-5 occurred, and this rod remained in the as-shipped condition.

Radiochemical analyses were performed for the six samples taken from SF-4, SF-8, and SF-12. Phase identifications were performed by X-ray diffraction (XRD) on separate fuel material and cladding samples. The key characterization results are summarized in Table S.1.

**Table S.1.** Summary of Key<sup>(a)</sup> Suspect Fuel Radiochemical Analysis and Phase Identification

Analyte	SF-4		SF-8		SF-12	
	Center	Near End	Center	Near End	Center	Near End
	SF-4-1	SF-4-2	SF-8-1	SF-8-2	SF-12-3	SF-12-2
<b>Concentration</b>	<b>µg/g Fuel Dissolved</b>					
U total	8.99E+05	8.94E+05	8.94E+05	9.03E+05	8.90E+05	8.98E+05
<sup>237</sup> Np	1.67E+00	1.60E+00	1.24E+00	7.85E-01	1.08E+00	7.38E-01
Pu total	4.20E+02	3.75E+02	2.93E+02	1.89E+02	2.74E+02	1.85E+02
<sup>241</sup> Am	2.92E-01	2.49E-01	9.69E-02	2.95E-02	<6.E-2	<3.E-2
<b>Concentration</b>	<b>µg/g Fuel Rod Segment<sup>(b)</sup></b>					
U total	7.67E+05	7.62E+05	7.58E+05	7.39E+05	7.37E+05	7.39E+05
<sup>237</sup> Np	1.43E+00	1.37E+00	1.05E+00	6.42E-01	8.93E-01	6.07E-01
Pu total	3.58E+02	3.19E+02	2.48E+02	1.55E+02	2.27E+02	1.53E+02
<sup>241</sup> Am	2.49E-01	2.12E-01	8.21E-02	2.41E-02	<5.E-2	<3.E-2
Cladding	1.46E+05	1.47E+05	1.52E+05	1.81E+05	1.66E+05	1.76E+05
Residual Solids <sup>(c)</sup>	4.51E+02	7.42E+02	4.04E+02	1.33E+03	9.57E+02	5.79E+03
<b>SNM Isotopic</b>	<b>Atom% of Element</b>					
<sup>235</sup> U	0.67	0.67	0.67	0.71	0.68	0.71
<sup>239</sup> Pu	97.71	97.93	98.27	98.66	98.58	98.96
<sup>240</sup> Pu	2.25	2.03	1.53	0.87	1.41	1.00
<b>SNM Isotopic</b>	<b>Wt% of Element</b>					
<sup>235</sup> U	0.66	0.66	0.66	0.70	0.67	0.70
<sup>239</sup> Pu	97.72	97.95	98.41	99.02	98.58	98.97
<sup>240</sup> Pu	2.26	2.04	1.54	0.88	1.42	1.00
<b>Gamma Activity</b>	<b>µCi/g Dissolved Fuel</b>					
<sup>137</sup> Cs, µCi/g	495	468	355	221	304	218
<sup>154</sup> Eu, µCi/g	0.0585	0.0469	<0.005	<0.004	<0.005	<0.003
<sup>60</sup> Co, µCi/g	0.0108	0.0113	0.00213	0.0314	<0.0009	<0.0007
<b>Phase Identification (XRD)</b>						
Fuel	UO <sub>2</sub>		UO <sub>2</sub>		UO <sub>2</sub>	
Cladding	Zr		Zr		Zr	

(a) More extensive characterization data, including radionuclide breakdown, are provided in Section 3.2.  
 (b) Fuel rod segment basis. Basis includes dissolved fuel, cladding, and residual solids for segment sample disk.  
 (c) Residual Solids are materials that did not dissolve during acid digestion in analytical preparation of the fuel.

The analyses for the suspect fuel items, SF-4, SF-8, and SF-12, are similar to each other. All three fuel rod items appear to contain slightly irradiated UO<sub>2</sub> fuel, originally of natural enrichment, with zirconium cladding. The uranium-235 isotopic concentrations decreased by the irradiation and became slightly lower than the natural enrichment of 0.72% to range from 0.67 to 0.71 atom%. The plutonium concentrations, as can be derived from Table S.1, ranged from about 206 to 467 grams per metric ton of uranium and ranged in <sup>239</sup>Pu concentration from about 97.7 to 99.0 atom%. The primary gamma emitter was <sup>137</sup>Cs, as would be expected for irradiated fuel.

During preparation for chemical analyses, the samples from all three fuel rod pieces showed similar dissolution behaviors. The cladding was unaffected by the dissolution process and the rinsed cladding rings were removed as the dissolution progressed. The dissolution process, however, left small quantities of residue that were not soluble in the mixed nitric/hydrochloric acid used for fuel dissolution. The

remaining residual solids, most likely bits of cladding from the fuel sectioning, contained little gamma or alpha activity in comparison with the fuel itself. With their relatively small quantities compared with the dissolved fuel and low relative weights, the residual solids were taken to be negligible contributors to the total nuclear material in the suspect fuel rods.

It also was observed for each rod piece that samples taken near the centers (SF-4-1, SF-8-1, and SF-12-3) had apparently endured more irradiation than the complementary samples taken from the fuel rod ends (SF-4-2, SF-8-2, and SF-12-2, respectively). Thus, the  $^{137}\text{Cs}$ ,  $^{154}\text{Eu}$ ,  $^{237}\text{Np}$ ,  $^{241}\text{Am}$ , and total plutonium concentrations are higher in the center samples than in the ends while the  $^{239}\text{Pu}$  and (generally)  $^{235}\text{U}$  atom% concentrations are lower. These differences are more pronounced for the SF-8 and SF-12 samples than for the SF-4 samples. The SF-4 fuel apparently underwent more irradiation than the SF-8 and SF-12 samples, whose irradiation exposures seemed to be similar based on their similar radionuclide concentrations.

Assuming irradiation in one of the Hanford production reactors, rough estimates of fuel irradiation exposure ranged from about 200 to 800 megawatt-days per metric ton of uranium. The best estimate of cooling time (time since discharge), based on the mole ratios of  $^{241}\text{Pu}$  to its daughter  $^{241}\text{Am}$ , is about  $30 \pm 6$  to  $42 \pm 14$  years (at one standard deviation). The fuel rod construction, dimensions, and materials and, to a lesser extent, the cooling times are consistent with items produced during N Reactor fuel development in the late 1950s.

The results of the analyses of the sections from three fuel rod pieces fulfilled the objectives specified by the SAP with no open issues. Therefore, no additional analyses were required of the fourth rod piece (SF-5) that had been reserved for contingent analyses.

## **Acknowledgements**

The authors would like to acknowledge the programmatic and technical oversight provided by Ron Baker, Darrel Duncan, and Kalli Shupe of the K Basin Closure Project, and Terri Welsh of Fluor Hanford Safeguards.

The authors would also like to gratefully acknowledge the support of other project staff at PNNL:

Suspect fuel receipt, inspections, physical characterization and sectioning/sampling were coordinated by Steve Halstead, Fran Steen, and Randy Thornhill.

The XRD sample preparations were performed by David Ortiz, the scans run by Matt Edwards, and the scans interpreted by Evan Jenson.

Digestions of the fuel segments were performed in the Shielded Analytical Laboratory by David Kallsen. The digested samples underwent radiochemical analyses performed by Larry Greenwood, Chuck Soderquist, Katharine Carson, Kathie Thomas, and Truc Trang-Le. The mass spectrometric analyses were run by Stan Bos, Pam Berry, and Lori Darnell.

Quality Engineering/Quality Assurance support was provided by Alice Lewis and Deborah Coffey.

## Contents

Summary .....	iii
Acknowledgements.....	vii
Terms and Acronyms.....	xiii
1.0 Introduction.....	1.1
2.0 Receipt, Physical Examinations, and Subsampling .....	2.1
2.1 Shipment and Receipt of Fuel at the RPL.....	2.1
2.2 Physical Inspections/Characterization .....	2.1
2.2.1 Initial Examinations .....	2.1
2.2.2 Detailed Examinations and Sectioning.....	2.5
3.0 Suspect Fuel Materials and Radiochemical Characterization Techniques and Results .....	3.1
3.1 X-Ray Diffractometry Measurements.....	3.1
3.1.1 X-Ray Diffractometry Sample Preparation and Analysis .....	3.2
3.1.2 X-Ray Diffractometry Results.....	3.2
3.2 Chemical and Radiochemical Analyses.....	3.5
3.2.1 Sample Dissolution and Digestion .....	3.5
3.2.2 Treatment and Analysis of Residual Solids.....	3.7
3.2.3 Solution Analysis Results.....	3.8
3.2.4 Mass-Based Concentrations .....	3.11
3.3 Interpretation of Chemical/Radiochemical Findings .....	3.13
4.0 Quality Assurance and Control Summary .....	4.1
5.0 References.....	5.1
Appendix A, Summary of In-Basin Characterization of Suspect Fuel Rod Pieces and Listing of Pieces Identified for Laboratory Analyses .....	A.1
Appendix B, Sectioning and Labeling Diagrams for Suspect Fuel Pieces, Remnant Piece Summary, and Calculations On Make-Up of Suspect Fuel.....	B.1



## Figures

2.1	Suspect Fuel Rod Pieces, from Top to Bottom, SF-12, SF-8, SF-5 and SF-4 .....	2.3
2.2	Tapered Cut End on SF-4 .....	2.3
2.3	Pin Fitting with Segment of Wire Wrap on SF-5.....	2.4
2.4	Flat Fitting on SF-8.....	2.4
2.5	Pin Fitting on SF-12.....	2.5
2.6	Sectioning of SF-12 with Low Speed Isomet Saw .....	2.6
3.1	XRD Scans for SF-4, SF-8, and SF-12 Cladding Samples and the Mounting Clay Blank.....	3.3
3.2	XRD Scans for SF-4, SF-8, and SF-12 Fuel Samples .....	3.4
3.3	Correlation of Plutonium Concentration to <sup>137</sup> Cs Concentration in Suspect Fuel Samples .....	3.14
B.1	Final Sectioning and Labeling Diagram for Suspect Fuel Rod Piece SF-4 .....	B.3
B.2	Final Sectioning and Labeling Diagram for Suspect Fuel Rod Piece SF-8 .....	B.3
B.3	Final Sectioning and Labeling Diagram for Suspect Fuel Rod Piece SF-12 .....	B.4

## Tables

S.1	Summary of Key Suspect Fuel Radiochemical Analysis and Phase Identification .....	iv
2.1	Suspect Fuel Rod Piece Identification Cross Reference Matrix .....	2.1
2.2	Physical Characterization Measurements of Suspect Fuel Rod Pieces.....	2.6
3.1	Fuel Cross-Section Sample Identification and Description .....	3.1
3.2	Digestion and Chemical/Radiochemical Analytical Procedures and SAP Sample QC Criteria.....	3.6
3.3	Fuel Sample Weights and Mass Balance .....	3.7
3.4	Suspect Fuel Radiochemical Analytical Results As-Reported .....	3.9
3.5	Suspect Fuel Radiochemical Analytical Results on Weight Bases.....	3.11
3.6	Isotope Properties .....	3.12
3.7	Calculated Plutonium Production in Seven-Rod Cluster Prototype Fuel of 1.3 and 1.6 Wt% <sup>235</sup> U Enrichment .....	3.15
3.8	Estimated Irradiation Exposure of Suspect Fuel Samples Based on Correlations for 1.3 and 1.6 Wt% Enriched Fuel Irradiated in the KE Reactor .....	3.16
3.9	Estimated Cooling Times Based on Relative <sup>241</sup> Pu and <sup>241</sup> Am Concentrations .....	3.16
A.1	Summary of In-Basin Characterization of Suspect Fuel Rod Pieces and Listing of Pieces Identified for Laboratory Analyses.....	A.3
B.1	Mass and Dimensions of Remnants After Suspect Fuel Sectioning.....	B.5

## Terms and Acronyms

Terms and acronyms used within this report are described below.

<b><u>Term</u></b>	<b><u>Explanation</u></b>
AEA	Alpha energy analysis
ASO	Analytical Support Operations
CoC	Chain of Custody
FH	Fluor Hanford, Inc.
GEA	Gamma Energy Analysis
HLRF	High Level Radiochemistry Facility (hot cells A-C) in the 325 Building
ICDD	International Centre for Diffraction Data
KBC Project	K Basin Closure Project
KPA	Kinetic phosphorescence analysis (for uranium)
KW	K West Basin
MCO	Multi-Canister Overpack
NIST	National Institute of Standards and Technology
PAS-1 cask	“Post-Accident Sample” cask - Multi-use shipping cask that has been approved for transport of nuclear fuel and sludge on the Hanford Site under special controls
PNNL	Pacific Northwest National Laboratory
OCRWM	Office of Civilian Radioactive Waste Management
RPL	Radiochemical Processing Laboratory (in 325 Building)
SAP	Sampling and Analysis Plan
SAL	Shielded Analytical Laboratory (lightly shielded hot cells in the 325 Building)
SSC	shielded sample container (special lead/stainless steel pig used in the PAS-1 cask for fuel and sludge, along with the corresponding inner rack for the PAS-1)
Suspect Fuel rod pieces	Fuel rod pieces in the KW Basin whose composition will be established through examinations and characterization at the 325 Building.
Suspect Fuel remnants	Suspect fuel rod pieces remaining after characterization and subsampling at the 325 Building. This fuel material must be returned to the KW Basin.
TIMS	Thermal ionization mass spectrometry
XRD	X-ray diffraction or diffractometry

## 1.0 Introduction

During the clean out of the 105 K West (KW) Basin, a group of 15 fuel rod pieces was found that could not be positively identified relative to source and composition based on the fuel geometry and lack of specific documentation (Ball 2005). Extensive review of the Hanford Site technical literature<sup>(a)</sup> (Sexton 2006) led to the postulation that these rod pieces likely were irradiated test fuel arising in support of the development of the Hanford “New Production Reactor”, later called N Reactor. Table A.1 (Appendix A) summarizes the limited information/data collected on the 15 “Suspect Fuel” rod pieces during underwater examinations/characterization at the KW Basin. The 15 suspect fuel rod pieces have lengths varying from 3 to 22 inches. Underwater masses ranged from less than a tenth of a pound (~45 g) to about 1.45 pounds (658 g). Underwater dose rate measurement performed with an RO-7 probe varied from 1 to 11 R/hr (on contact) relative to the underwater background dose rate of ~1 R/hr. Based on their geometries and underwater weights, the densities of the rod pieces were calculated. One rod piece exhibited a density consistent with uranium metal, while nine others had densities consistent with uranium oxide and four evidently were “empty” cladding (i.e., indicating minimal fuel). The remaining rod piece, believed to contain uranium metal, was dropped in an area on the KW Basin floor that cannot be accessed until large scale equipment is removed when KW is finally cleaned out.

A Sampling and Analysis Plan (SAP) (Baker et al. 2006) was developed to establish the framework for characterization of the suspect fuel so that rod pieces containing significant fuel can be placed in Multi-Canister Overpacks (MCO) for dispositioning along with other spent nuclear fuel from K Basins. Under the SAP, 4 rod pieces from the population of 15 were selected for shipment to the Pacific Northwest National Laboratory (PNNL) Radiological Processing Laboratory (RPL) (also known at the 325 Building). The rod pieces chosen for characterization were selected to be generally representative of the oxide fuel in the population and capable of fitting into the shipping container without in-basin size reduction. Lengths thus were limited to about 14 inches. The SAP specified that 3 of the 4 suspect fuel rod pieces shipped to the 325 Building were to be subjected to examination and characterization. The fourth rod piece was to serve as a contingency in the event that the samples from an additional rod piece would be required. The SAP specifications were based in-part on the expectation from the extensive literature reviews of historic Hanford documents that the oxide fuel rod pieces are from one general population (Baker et al. 2006).

Within the SAP, the primary objectives of the fuel characterization effort were identified:

- 1) determination of the nuclear materials accountability values for the suspect fuel rod pieces being loaded into the MCO
- 2) generation of sufficient information to demonstrate that including the suspect fuel rod pieces in an MCO will not increase risk that the Office of Civilian Radioactive Waste Management (OCRWM) will not accept this MCO for off-site transport or final disposition at the federal High Level Waste (HLW) repository.

---

(a) PNNL letter report 50129-RPT02, “Technical Literature Investigation of the Source of the KW Basin Suspect Fuel,” prepared by CH Deleгарd (PNNL) and transmitted via letter 50129-L02 by PA Scott (PNNL) to DR Duncan (FH) on December 16, 2005.

To meet these objectives, the specific minimum laboratory analyses required that the fuel composition be determined (i.e., plutonium and uranium concentrations, uranium enrichment, plutonium isotopes, and radionuclide isotopic content) and that the cladding material be identified (e.g., stainless steel, zircaloy, etc.).

The characterization results from examinations and laboratory analyses performed (consistent with the SAP) on the subset of fuel rod pieces at the RPL are summarized in this report. The receipt, inspections, physical characterization, and subsampling of the suspect fuel rod pieces are described in Section 2.0. Section 3.0 describes the dissolution of the fuel (analytical preparation), and presents the results of the phase identification (X-ray diffraction analysis) and radiochemical analysis. Discussion and interpretation of the characterization results are also provided in Section 3.0. Quality assurance measures are described in Section 4.0. Appendix A includes the results from the prior in-basin characterization of the suspect fuel population performed by the K Basin Closure (KBC) Project. Appendix B provides the final subsampling or cut diagrams for the three suspect fuel rod pieces that were analyzed, a summary of remnant pieces remaining after rod piece sectioning, and calculations on the make-up of suspect fuel.

A technical data package containing the Chain of Custody (CoC) form, completed test instructions, laboratory data summary reports, and the raw data is maintained in the PNNL project records and has been provided to Fluor Hanford (FH) [KBC Project records, FH Safeguards (T. L. Welsh), and KBC Engineering (R. B. Baker and D. R. Duncan)]. Videotape was collected during the physical examinations and sectioning of the suspect fuel rod pieces. Copies of these videotapes were provided to FH (R. B. Baker) and will be retained by PNNL project staff (A. J. Schmidt).

## 2.0 Receipt, Physical Examinations, and Subsampling

The receipt, physical examinations, and subsampling of the suspect fuel occurred at the RPL after shipment from the KW Basin.

### 2.1 Shipment and Receipt of Fuel at the RPL

Based on guidance provided in the SAP, four pre-selected suspect fuel rod pieces (designated as #4, #5, #8 and #12) were verified as to identity and loaded underwater at the KW Basin into a special fuel basket, which was then placed into a special lead/stainless steel pig [referred to as the shielded sample container (SSC)]. Next, the SSC, containing the fuel rod pieces and water, was removed from the KW Basin pool, bagged, and then placed in a Hanford PAS-1 cask. The loaded cask was received at the RPL on April 6, 2006, with a CoC to document the transfer of the fuel from FH to PNNL. The fuel shipment was performed under the provisions of “One-Time Request for Shipment Spent Nuclear Fuel Coupons in the PAS-1 Cask” (Fluor 2006). On April 12, 2006, after being recovered from the PAS-1 cask, the SSC was drained of water, and the suspect fuel rod pieces were offloaded into a hot cell (A-Cell) within the High Level Radiochemistry Facility (HLRF) at the RPL.

Table 2.1 provides a cross-reference matrix of the identification nomenclature for the suspect fuel rod pieces shipped to the 325 Building.

**Table 2.1.** Suspect Fuel Rod Piece Identification Cross Reference Matrix

<b>Chain of Custody Identification</b>	<b>Sampling and Analysis Plan Identification</b>	<b>Identification Used at the RPL</b>
SFP-06-004	#4	SF-4
SFP-06-005	#5	SF-5
SFP-06-008	#8	SF-8
SFP-06-012	#12	SF-12

### 2.2 Physical Inspections/Characterization

Physical inspections of the suspect fuel occurred in the HLRF.

#### 2.2.1 Initial Examinations

Upon offloading the suspect fuel rod pieces into the HLRF, initial examinations were conducted to confirm the identities of each rod piece and to obtain information and videotape records to establish subsampling plans (i.e., cutting diagrams). The rod pieces were identified based on pictures included within the SAP and within PNNL Test Instructions because the rod pieces do not have unique numbering. The rod pieces were videotaped, measured for length and diameter, weighed, and placed into their respective pipe storage containers. For each rod piece, a reference dimensional scale and color reference card were included during a portion of the videotaping. Measurements and notes from the initial

examinations were documented in project-specific test instructions which are included in the PNNL technical data package.

The appearance and weights of the suspect fuel rod pieces were generally consistent with those projected based on the previous underwater measurements performed at the KW Basin (Baker et al. 2006). Figure 2.1 shows the four rod pieces in the HLRF.

Observations from the initial examinations are summarized below:

SF-4 Both ends of the fuel rod piece exhibit oblique tapered cuts with solid material (inferred to be fuel) extending and visible on both ends. The solid material was black, granular/crystalline in appearance, and had surfaces that reflected light. No brown or yellow color was observed on the solid material, which could have been indicative of higher oxidation states of uranium. Figure 2.2 is a close up view of a taper-cut end on SF-4. Fuel was visible  $\frac{7}{8}$  inch from one end, and  $1\frac{3}{16}$  inches from the other end. A crack in the cladding on one of the tapered cuts was visible. The cladding surface was oxidized (mottled appearance) and some small pits were visible. Markings on the cladding gave evidence that the rod had been wire-wrapped with a pitch of approximately 1 wrap per foot.

SF-5 One end of SF-5 exhibited a pin fitting with a length of wire wrap still attached (Figure 2.3). The distance from the end of the pin fitting to where fuel was assumed to start is  $\frac{3}{8}$  inch. The other end the cladding was broken, with jagged edges exposed. Black solid material (similar to that observed in SF-4), inferred to be fuel, was observed approximately  $\frac{1}{2}$  to  $\frac{5}{8}$  inch inside of the broken end. The cladding surface was apparently oxidized (mottled appearance), with green areas in several spots, and some small pits were visible. Marks from wire wrap were seen but were insufficient to estimate pitch.

SF-8 One end of SF-8 was closed with a flat fitting or end cap and the other end was neatly cut. The end cap was notched with what appeared to be a **v** or **y** pattern (see Figure 2.4). The pinched or indented cladding wall cut likely was made using a tubing cutter. Solid material (similar to that seen in other rod pieces), inferred to be fuel, was observed inside the cladding  $\frac{3}{8}$  inch inside of the cut end. The cladding surface condition was similar to the other rod pieces, although scratch marks and marks from pliers or a vice type tool were observed. With the marred surface, no distinct patterns left from a wire wrap could be identified.

SF-12 One end of SF-12 exhibited a pin fitting (e.g., end cap) with a short length of wire wrap (Figure 2.5). The other end of the rod piece was bent and the end had neatly cut cladding walls at an angle such as might be made by a tubing cutter. Solid material (similar to that seen in other rod pieces), inferred to be fuel, was observed inside the cladding at a depth of  $\frac{1}{4}$  inch from the bent end. The cladding surface condition was similar to the SF-4 and SF-8. Like SF-5, marks from wire wrap were found but the pitch could not be estimated.

The initial inspections were conducted with the fuel rod pieces laid out on a clean white towel. After the inspections were completed, no particulate debris was observed on the towel.



**Figure 2.1.** Suspect Fuel Rod Pieces, from Top to Bottom, SF-12, SF-8, SF-5 and SF-4. SF-12 is approximately 13.3 inches long, and SF-4 is approximately 9.9 inches long.



**Figure 2.2.** Tapered Cut End on SF-4





**Figure 2.3.** Pin Fitting with Segment of Wire Wrap on SF-5



**Figure 2.4.** Flat Fitting on SF-8. Note the apparent v or y pattern of notch on fitting.



**Figure 2.5.** Pin Fitting on SF-12

## 2.2.2 Detailed Examinations and Sectioning

After completing the initial examinations, cut plans were finalized for obtaining analytical subsamples from rod pieces SF-4, SF-8, and SF-12. Appendix B provides diagrams that depict the as-sectioned fuel rod pieces. A cut plan was also formulated for SF-5, but was not executed. Additional physical characterization was also completed to document the dimensions (measured with a dimensional scale) and masses of the fuel rod pieces before subsectioning. Daily linearity checks were performed on balances. Rod piece diameters were measured using uncalibrated dial calipers. Before the measurements were made, the calipers were set to zero (operation was videotaped). The diameter measurements were generally consistent with measurements performed using a dimensional scale and agreed with previous underwater measurements (Appendix A). Table 2.2 summarizes the physical measurements, and includes the mass of the remnants remaining from each fuel rod piece after subsectioning. [Additional mass and length information on the remnant pieces is provided in Appendix B.]

For radiochemistry analysis, two  $\sim\frac{1}{8}$ -inch thick disks samples were cut from each of the three primary suspect fuel rod pieces (SF-4, SF-8, and SF-12). For SF-12, a sample solution was lost during dissolution (vial slipped during analytical preparation); therefore, a third sample disk was taken from the rod material. Figure 2.6 shows the cutting of a section from SF-12. One sample disk was taken from each rod near the center and a second sample from each rod was taken  $\sim 2$  inches from an end. An additional disk ( $\sim\frac{1}{8}$ -inch thick) was also obtained from near the center of each rod to provide sample material for X-ray diffraction (XRD) analysis of fuel and cladding. Attempts to pick a piece of fuel from the sample disk or free the fuel from the cladding ring were unsuccessful (i.e., fuel exhibited significant structural integrity and bonding to the cladding). Therefore, for the XRD sub-samples where a small portion of fuel and cladding material were required, the sample disk was cut in half.

**Table 2.2.** Physical Characterization Measurements of Suspect Fuel Rod Pieces

Parameter	Suspect Fuel Rod Piece			
	SF-4	SF-8	SF-12	SF-5 <sup>(a)</sup>
Dry Mass, g (as received)	292.8	444.3	449.2	292.7
Overall Length, inches	9.88	13.0	13.31	9.25
Fueled Length, <sup>(b)</sup> inches	7.81	12.5	12.69	8.31
Diameter, inches	0.55	0.55	0.56	NM <sup>(c)</sup>
Cladding thickness, <sup>(d)</sup> inches	0.031	0.031	0.031	NM <sup>(c)</sup>
Mass per Fueled Length, <sup>(e)</sup> g/axial inches (fueled section)	36.5	36.4	36.5	NM <sup>(c)</sup>
Mass, remnant pieces, <sup>(f)</sup> after sectioning, g	278.6	431.2	429.3	292.7
<p>(a) SF-5 was held in contingency, and was not sectioned.</p> <p>(b) Length of rod piece occupied by fuel (it is assumed all solid material observed was fuel). Estimates were made of where fuel begins on closed ends of rod pieces (see Appendix B).</p> <p>(c) NM = not measured</p> <p>(d) Prior to sectioning, cladding thickness was estimated to be approximately 1/32 (or 0.031) inch. This estimate is consistent with examinations of post sectioning photos.</p> <p>(e) Calculated based on one of the completely fueled remnant segments cut from mid-section of rod pieces (see Table B.1). Some variation in mass per length throughout the fuel column is expected, leading to potential slight variations in estimating total fuel column mass.</p> <p>(f) Total mass of remnant pieces to be returned to the KW Basin.</p>				



**Figure 2.6.** Sectioning of SF-12 with Low Speed Isomet Saw. Water is being used a coolant/cutting lubricant. The outside diameter of SF-12 is 0.55 to 0.56 inch. A portion of the circular saw blade is shown below the fuel.

Sectioning of the suspect fuel rod pieces was performed using a Buehler Low Speed Isomet saw, modified for in-cell use. A diamond wafering blade [Buehler Series 15, HC (high concentration) Diamond blade] was used for all cutting and water was used as a coolant/lubricant. Use of water during cutting provided faster and cleaner cuts (minimizing fuel crumbling and chipping) and controlled the spread of fuel dust. To minimize cross contamination, the saw blade was replaced or cleaned between sectioning the fuel rod pieces. One end of each rod piece was selected as the reference end and nicked with the saw blade to mark and maintain orientation with the cut plan. Rod segments that were devoid of obvious reference points were also nicked on one end to mark orientation. The cut plans, notes, and measurements from fuel sectioning were documented directly into the controlled copy of the test instructions.

The rod sectioning method (i.e., saw, blade, use of water, etc.) was based on prior PNNL experience with sectioning irradiated fuel pins for other projects. The sectioning of the KBC suspect fuel rod pieces was performed very efficiently. The cladding and fuel were cut cleanly and a typical transverse diametral cut of fuel/cladding was performed in about 3 to 5 minutes. Minimal small loose fuel pieces were observed during the cutting. Generally the fuel material was observed to be dark grey to black in color and have apparent open interconnected porosity. Light spots noted in images of the fuel cross-sections (see Figure 2.6) are reflections of light off the various small surfaces of the material making up the fuel. Similar observations were made during prior in-basin examinations at KW. The fuel material appeared to be in intimate contact with the cladding inner diameter with no looseness (i.e., there was no apparent open fuel-to-cladding gap). No unique bonding material (or evidence of prior existence of bonding material) was observed between the bulk fuel outer diameter and inner cladding diameter.

### 3.0 Suspect Fuel Materials and Radiochemical Characterization Techniques and Results

Material and radiochemical characterizations were performed on the portions of three of the suspect fuel rod items numbered SF-4, SF-8, and SF-12. The sample portions were collected during subsectioning activities in the HLRF as described in Section 2.2.2, and were transferred to the Shielded Analytical Laboratory (SAL) for further preparation. Three types of samples were collected from each fuel rod:

- small ( $\sim 1/8$ -inch  $\times$   $3/16$ -inch) pieces of cladding
- small particles of fuel
- two  $\sim 1/8$ -inch thick transverse sawn cross-sections of fuel rod with cladding.

The cladding pieces and small fuel particles were collected for phase identification by XRD. The transverse cross-sectional samples were taken for chemical and radiochemical analyses of the fuel contained within the cladding. The identification numbers and locations from which the cross sectional samples were taken are described in Table 3.1.

**Table 3.1.** Fuel Cross-Section Sample Identification and Description

Sample ID	ASO <sup>(a)</sup> Sample ID	Sample Description
SF-4-1	06-01386	Sample section from middle (axially) of SF-4.
SF-4-2	06-01387	Sample section taken $2\frac{7}{8}$ inches from reference end. Axial distance between SF-4-1 and SF-4-2 approximately $2\frac{1}{4}$ inches.
SF-8-1	06-01388	Sample section from middle (axially) of SF-8.
SF-8-2	06-01389	Sample section taken $2\frac{3}{8}$ inches from reference end with flat fitting. Axial distance between SF-8-1 and SF-8-2 approximately $3\frac{3}{4}$ inches.
SF-12-1	06-01390	Sample section from middle (axially) of SF-12. Solution prepared from this sample subsequently was lost during manipulation in the hot cell. The sample SF-12-3 was taken for analysis to replace SF-12-1.
SF-12-3	06-01420	Sample section from middle (axially) of SF-12 taken to replace SF-12-1.
SF-12-2	06-01391	Sample section taken $1\frac{7}{8}$ inches from reference end with pin fitting. Axial distance between SF-12-2 and SF-12-3 approximately $4\frac{1}{2}$ inches.
(a) ASO is Analytical Support Operations.		

The results from the XRD and the chemical/radiochemical analyses are reported, respectively, in Sections 3.1 and 3.2. Some generalizations and interpretations from the analytical findings are presented in Section 3.3.

#### 3.1 X-Ray Diffractometry Measurements

One sample of cladding and one sample of fuel were taken from each of the three tested suspect fuel rod pieces, SF-4, SF-8, and SF-12. The analytical methods and sample phase identification results are described in this section.

### 3.1.1 X-Ray Diffractometry Sample Preparation and Analysis

The cladding and particle samples were taken for characterization by XRD. The XRD technique was used to identify crystalline phases in the cladding and fuel particles. Samples were prepared for XRD analyses following standard RPL procedures.<sup>(a)</sup>

Each of the cladding samples were slightly curved because of their origin from the cylindrical suspect fuel rods. Each sample was mounted intact, convex-upward, on adhesive paper which, in turn, was mounted on adhesive clay. Each sample on paper was pressed into the clay until the upper part of the curved surface was in the calibrated plane of the sample mount. In this orientation, the outer surface of the fuel rod (water side) was interrogated by the X-ray beam. The cladding sample mounts then were covered with a Kapton-windowed plastic sample holder and glued at all seams for radioactive contamination control. Kapton is a high strength polyimide that is X-ray translucent and X-ray indifferent (i.e., has no distinct X-ray pattern) and used in a film form in this application.

The fuel samples were crushed and ground to fine powders in the hot cell using a mortar and pestle. Each powder was blended with a portion of Al<sub>2</sub>O<sub>3</sub> (corundum) powder, Standard Reference Material 674, obtained from the National Bureau of Standards (NBS; this organization is now called the National Institute of Standards and Technology, or NIST). The Al<sub>2</sub>O<sub>3</sub> powder was used as an internal standard to calibrate the diffraction angle. The fuel particles were friable and crushed without undue effort. The fuel and Al<sub>2</sub>O<sub>3</sub> powders were crushed and blended as slurries in an isoamyl acetate solution of collodion. Each blended slurry then was pipetted onto a glass microscope slide and allowed to cure, drying to form a film of the mixed powders. The slides were removed from the hot cell, wrapped in thin foils of Kapton, and taped for contamination control.

Both the metal cladding and the powder fuel samples were analyzed by an established RPL procedure<sup>(b)</sup> on a Scintag PAD V X-ray diffractometer. The XRD scans were gathered using copper K<sub>α</sub> X-radiation over the range 20 to 50 degrees, 2-θ (theta), with 0.02-degree step size and a counting time of 2.0 seconds per step. The scans were evaluated with the aid of JADE software (version 7.5, Materials Data Inc., Livermore, CA) and the peaks compared with the PDF-2 release 2005, version 2.05, International Centre for Diffraction Data (ICDD) powder diffraction file library to help identify phases in the samples.

### 3.1.2 X-Ray Diffractometry Results

#### *Cladding*

The XRD scans for the three cladding samples, given in Figure 3.1, are adjusted in the y-axis to allow their ready comparison. The scans are presented with a background blank scan of the clay that was used as a pliable adhesive to hold the adhesive paper (Post-it note paper) on which each cladding sample was mounted.

---

(a) RPL-PIP-4, Rev. 4, "Preparing Sealed Radioactive Samples for XRD and Other Purposes."

(b) PNNL-RPG-268, Rev. 2, "Solids Analysis, X-Ray Diffraction."

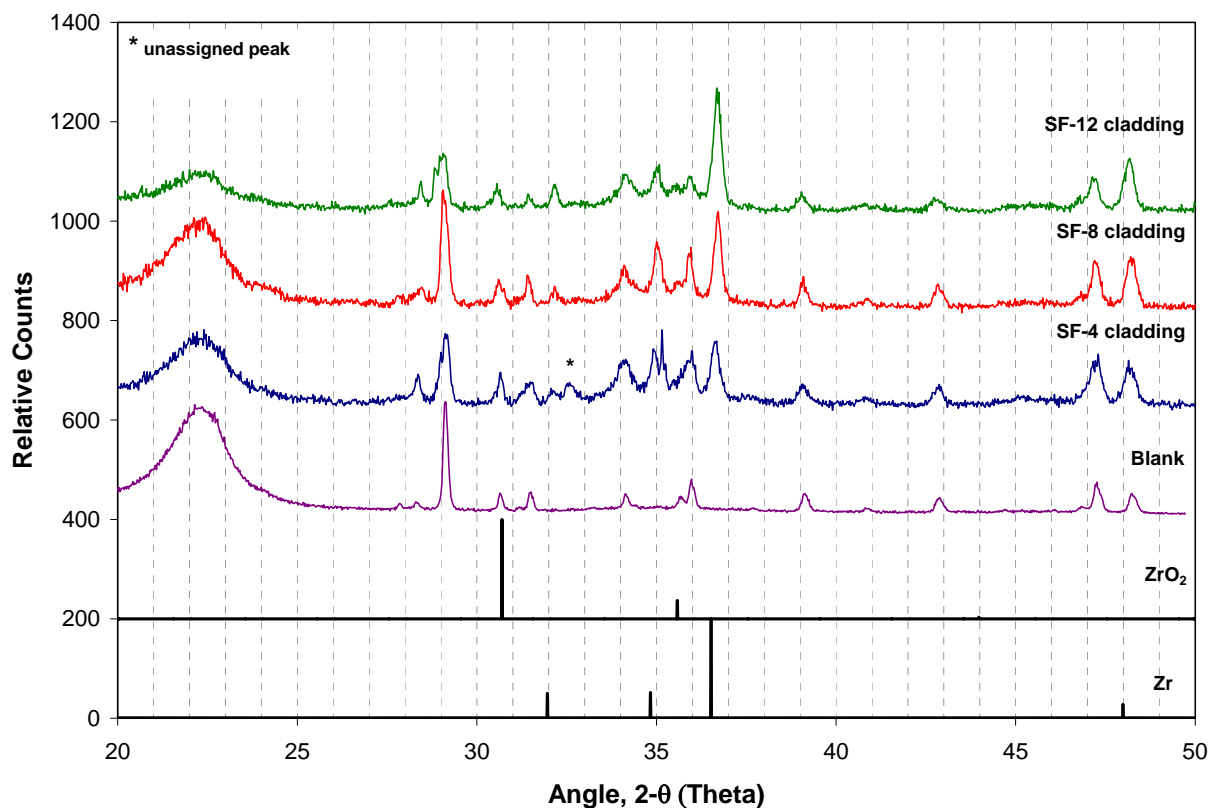


**Figure 3.1.** XRD Scans for SF-4, SF-8, and SF-12 Cladding Samples and the Mounting Clay Blank

It is seen that the scans for the three cladding samples are remarkably similar and that the mounting clay (blank) provided a number of prominent peaks to all of the scans. By visual comparison, however, it can be seen that peaks are present in the cladding scans that are not present in the clay. The most conspicuous of the non-clay peaks appear at about 32.1, 35.0, and 36.7 degrees 2-θ. These peaks are displaced about 0.1 degrees to higher 2-θ from the most prominent peaks for zirconium metal at 32.0, 34.8, and 36.5 degrees 2-θ as seen by comparison with the “stick figure” diffraction pattern for zirconium, also given in Figure 3.1. Another (but weaker) peak for zirconium at 48.0 degrees 2-θ is overlain by a clay peak. Given the curved surface of the fuel cladding, which certainly caused peak shifting and broadening, this coincidence of peak locations allows a confident identification of the cladding phase as zirconium for all three samples, SF-4, SF-8, and SF-12.

Zirconium dioxide, ZrO<sub>2</sub>, also might be expected to be present on the surface of the zirconium cladding and be identifiable by XRD. Indeed, as found by visual observation in the SAL, each of the cladding samples had the shiny black ZrO<sub>2</sub> patina that is found for zirconium that has been passivated in steam, high temperature liquid water, or furnace treatment in air. However, the XRD pattern for ZrO<sub>2</sub> has only two peaks in the range 20-50 degrees 2-θ, and both of these peaks coincide with peaks from the underlying clay. Therefore, a positive identification of ZrO<sub>2</sub> in the SF-4, SF-8, or SF-12 samples cannot be made based on the XRD data.



A single additional peak that cannot be assigned to the clay, to zirconium metal, or to  $ZrO_2$  appears for the SF-4 cladding at about 32.6 degrees  $2\theta$  (indicated by the asterisk in Figure 3.1). Identification of a phase based on this single peak cannot be made with confidence.

### Fuel

The XRD scans for the three fuel particle samples are shown in Figure 3.2. The three scans, displaced from each other in the y-axis to allow comparison, are remarkably similar. The XRD stick figure for  $Al_2O_3$ , also given in Figure 3.2, shows the locations, at about 25.6, 35.1, 37.8, and 43.3 degrees  $2\theta$ , of the internal standard peaks in the scans for the fuel samples. The three remaining prominent peaks at 28.2, 32.7, and 46.9 degrees  $2\theta$  are fit very well by uranium dioxide,  $UO_2$ , as seen by comparison with the stick figure diffraction pattern for  $UO_2$ .

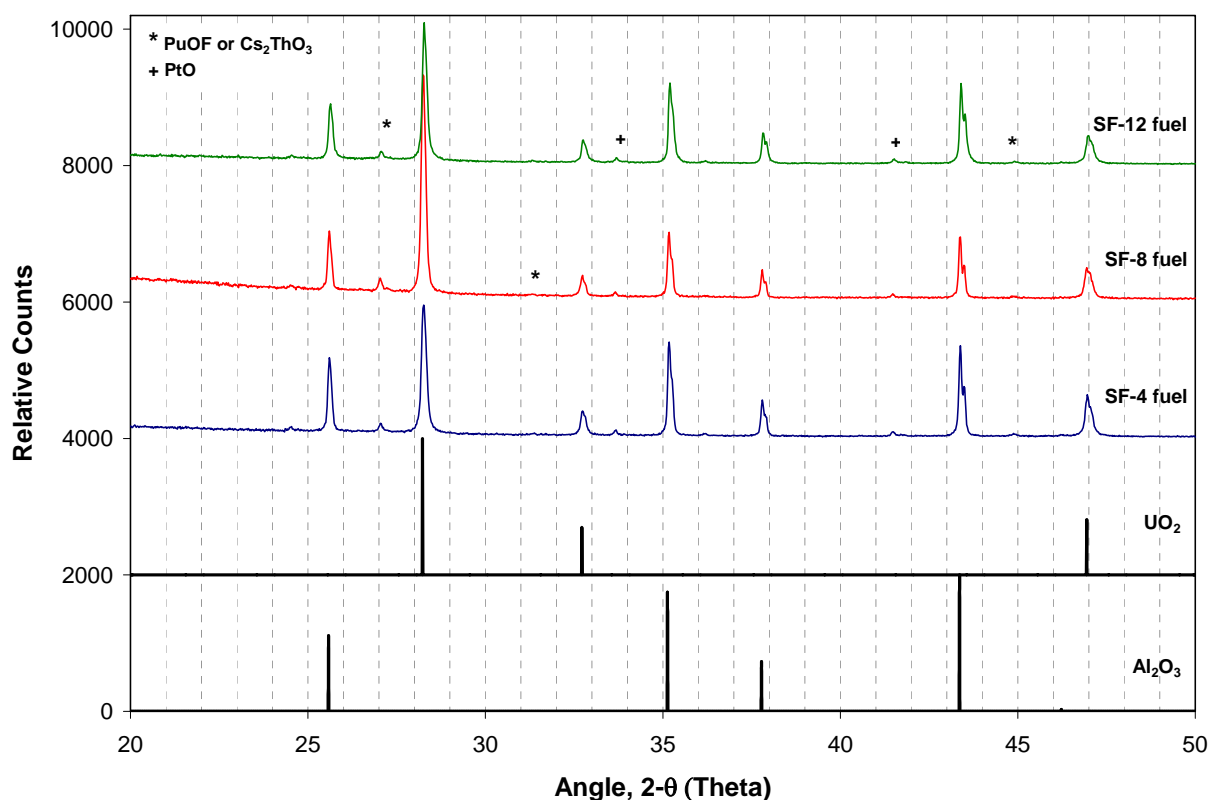


**Figure 3.2.** XRD Scans for SF-4, SF-8, and SF-12 Fuel Samples

Five other small peaks, at about 27.1, 31.3, 33.7, 41.5, and 44.9 degrees  $2\theta$ , are seen in most scans. Assignment of these peaks to higher uranium oxides was not successful. Such oxides might be expected from oxidation of the fuel underwater or by air. However, the fuel samples taken for XRD were retrieved from the interior of the fuel rods and were only exposed to water for brief periods during cutting. The peaks also do not correspond to zirconium or  $ZrO_2$ .

Based on survey of the ICDD XRD files, the peaks were most closely fit by plutonium oxide fluoride,  $PuOF$ , or cesium thorium oxide,  $Cs_2ThO_3$ , and by platinum oxide,  $PtO$ . The peaks associated with these



phases are indicated in Figure 3.2. None of these three phases are consistent with the chemical analyses as presented in the following section of this report. Isomorphous uranium analogs of the two actinide phases, i.e., UOF for PuOF and  $\text{Cs}_2\text{UO}_3$  for  $\text{Cs}_2\text{ThO}_3$ , may be suggested. However, the preparations of ternary oxides of the composition  $\text{M}_2\text{UO}_3$  have not been successful and the existence of compounds like  $\text{Cs}_2\text{UO}_3$  in the suspect fuel is unlikely. Keller (1972) states, "It therefore seems very improbable that alkali metal uranates(IV) . . . exist." Similarly, no evidence for the existence of UOF was found in the technical literature. Therefore, no definitive phase assignments may be made based on these minor peaks.

Hence, both the cladding and fuel have minor potential phases that are not definitely identified with this analytical method. The base primary indicated phases composing the cladding and fuel are identified. It is not unusual for XRD analyses to have "unknowns" when evaluating real world materials from the field.

## 3.2 Chemical and Radiochemical Analyses

Chemical and radiochemical analyses performed on the fuel materials present in the six transverse cross-sections taken (two each) from the three analyzed suspect fuel items were made in accordance with the SAP requirements and the ASO QA Plan.<sup>(a)</sup> The locations of the six samples are described in Table 3.1. The chemical and radiochemical analyses were performed according to established analytical procedures and began with a stepwise digestion of the fuel materials in acid. The procedures used in the digestion and analyses, and the SAP sample QC criteria, are described in Table 3.2. The cross-sectional fuel sample weight data are presented in Table 3.3.

### 3.2.1 Sample Dissolution and Digestion

The sample disks cut from the suspect fuel were first heated to constant weight to drive out any water remaining from the cutting operation. Because the material(s) of construction of the cladding were not known, the acid digestions of the fuel sample sections were undertaken in a graded fashion. The dissolution procedure, as written, called for mixed 4 molar (M) nitric acid ( $\text{HNO}_3$ ) and 4 M hydrochloric acid (HCl). The mixed  $\text{HNO}_3/\text{HCl}$  solution would have attacked stainless steel, a potential cladding material, or other iron-based alloys. Instead, 4 M  $\text{HNO}_3$ , which does not significantly attack stainless steel, was used first without any added HCl.

The samples with portions of 4 M  $\text{HNO}_3$  were heated in polypropylene vials to about 95°C. The acid and samples were observed to react during heating, releasing bubbles and forming a yellow solution as would be expected for the reaction of uranium or  $\text{UO}_2$  with  $\text{HNO}_3$ . A video camera inside the hot cell was used to make the detailed visual observations. The cladding, however, remained apparently unaffected by the acid treatment. The acid was added in several portions, with heating, until only the cladding and a small amount of small black particulate solids remained undissolved. A total volume of 28 milliliters (ml) of 4 M  $\text{HNO}_3$  was added but the final solution volumes were lower due to evaporation.

The cladding from each cross-sectional rod sample had the form of a ring. The rings were retrieved from each digestion vial, rinsed with deionized water with the rinsate collected in the digestion vials, and dried to constant weight. The cladding weights are shown in Table 3.3. Each cladding ring appeared to be free of residual fuel and had a shiny black patina on its outer surface. The inside of the rings, i.e., next to the fuel, appeared to be slightly pitted or scored. The cut surfaces of the cladding rings showed burrs.

---

(a) ASO-QA-001, Rev. 4, "Analytical Support Operations (ASO) Quality Assurance Plan."

**Table 3.2.** Digestion and Chemical/Radiochemical Analytical Procedures and SAP Sample QC Criteria

Analysis Objective	Procedure Number	Procedure Title	Req. Method Detection Limit (MDL)	Preparative Duplicate (Precision)	Blank Spike (Accuracy) <sup>(a)</sup>	Calib. Verif./ Counter Control <sup>(b)</sup>	Lab Prep. Duplicates <sup>(c)</sup> per Batch
Acid Digestion	PNL-ALO-129	HNO <sub>3</sub> -HCl Acid Extraction of Solids Using a Dry-Block Heater	NA	NA	NA	NA	NA
U/KPA <sup>(d)</sup>	RPG-CMC-4014	Uranium by Kinetic Phosphorescence Analysis	10 µg/g	± 20%	± 20%	± 7.5%	1
U-TIMS <sup>(e)</sup>	RPG-CMC-455	Separation of Uranium and Plutonium for Isotopic Analysis by Mass Spectrometry	NA	± 20%	± 20%	± 2%	1
	PNNL-98523-264	Mass Spectrometer Isotopic Analysis					
Total Pu – AEA <sup>(f)</sup>	RPG-CMC-455	Separation of Uranium and Plutonium for Isotopic Analysis by Mass Spectrometry	5.0 µCi/g	± 20%	± 20%	[See Section 4.1] <sup>(h)</sup>	1
	RPG-CMC-496	Coprecipitation Mounting of Actinides for Alpha Spectroscopy					
	RPG-CMC-422	Solutions Analysis: Alpha Spectrometry					
Pu – TIMS <sup>(e)</sup>	RPG-CMC-455	Separation of Uranium and Plutonium for Isotopic Analysis by Mass Spectrometry	NA	± 20%	± 20%	± 2%	1
	PNNL-98523-264	Mass Spectrometer Isotopic Analysis					
Am-241 – GEA <sup>(g)</sup>	RPG-CMC-450	Gamma Energy Analysis (GEA) and Low-Energy Photon Spectrometry (LEPS)	15.0 µCi/g	± 20%	± 20%	2 sigma (SPC)	1
Np – AEA <sup>(f)</sup>	PNL-ALO-4015	Analysis of Soil and Sediment Samples for Actinides and Sr-90	5.0 µCi/g	± 20%	± 20%	[See Section 4.1] <sup>(h)</sup>	1
	RPG-CMC-422	Solutions Analysis: Alpha Spectrometry					

(a) All matrix spike recoveries should be within 25%.  
 (b) Counter instruments will be checked daily with counter control samples to ensure performance is within statistical process control criterion of 2-sigma SPC (Statistical Process Control).  
 (c) Laboratory preparative duplicate is an aliquot of one of the original samples processed in duplicate through the preparative processes.  
 (d) KPA is Kinetic Phosphorescence Analysis.  
 (e) TIMS is Thermal Ionization Mass Spectrometry.  
 (f) AEA is Alpha Energy Analysis.  
 (g) GEA is Gamma Energy Analysis.  
 (h) In accordance with ASO QA Plan, post preparative blank and matrix spikes were performed for Pu-AEA and Np-AEA. Additionally for Pu-AEA, an isotopic tracer (internal standard) was added to each sample.

**Table 3.3.** Fuel Sample Weights and Mass Balance

Sample ID	Gross Sample Weight, g	Cladding Weight, g	Residual Solids Weight, g	Net Weight Dissolved Fuel, g	Residual Solids, Wt% of Fuel
SF-4-1	4.4309	0.6484	0.0020	3.7805	0.053
SF-4-2	4.4450	0.6525	0.0033	3.7892	0.087
SF-8-1	4.2130	0.6397	0.0017	3.5716	0.048
SF-8-2	3.7566	0.6781	0.0050	3.0735	0.162
SF-12-3	3.9345	0.6533	0.0228	3.2584	0.695
SF-12-2	4.0734	0.7180	0.0039	3.3515	0.116

The solution samples with black residual particulate solids were treated by the addition of 8 ml of 4 M HCl to the original HNO<sub>3</sub> and left for three days at cell temperature (~30°C). The residual solids were apparently unaffected after the three-day contact. The samples then were heated to ~95°C for two hours. Still, no additional dissolution was observed. At this point, the contents of the vial for one of the SF-12 samples (the sample was designated as SF-12-1) were spilled during handling. A replacement sample (designated SF-12-3; see Table 3.1) was taken from the remaining material from this rod, dried to constant weight, and treated with 25 ml of HNO<sub>3</sub> to bring this sample to the same point as the remaining five undisturbed samples.

As seen in the next section, efforts to dissolve the residual solids were unsuccessful. Because the radionuclide concentrations in the undissolved residues were small, it was decided to separate the solutions from the residual solids. The residual solids were rinsed and the rinses added to the dissolved fuel. The solutions for all six samples, separated from the cladding rings and the residual solids, then were treated with roughly equal volumes of 4 M HCl. The solutions weights and densities were measured and the solutions analyzed for uranium and radionuclide concentrations according to the procedures given in Table 3.2.

### 3.2.2 Treatment and Analysis of Residual Solids

In the mean time, the residual solids from the lost sample SF-12-1 were used to test dissolution methods. In the first attempt, the solution was removed from the salt-and-pepper colored residual solids and a mixture of 3-parts HCl and 1-part HNO<sub>3</sub>, both as their concentrated reagents (i.e., aqua regia), were added to give about 1-ml total solution volume. No apparent solids dissolution was observed even after 1-hour heating at 95°C. The solution was removed and another portion of aqua regia added to the vial with solids. Again, however, 3-hours of contact at cell temperature failed to dissolve any additional solids.

The solution was removed by pipet and ~50 microliters (μl) of concentrated hydrofluoric acid (HF) added. The video camera was placed to view the flat bottom of the digestion vial so that any reaction signs (bubbling, swirling, solids disappearance or growth) could be readily seen. Again, however, there was no apparent reaction. Two drops (about 100 μl) of concentrated (~16 M) HNO<sub>3</sub> were added to the vial with residual solids and HF. No reaction was observed. Then, 2-ml of concentrated HNO<sub>3</sub> and 4-ml of water were added to the vial. This would make ~5 M HNO<sub>3</sub> and ~0.24 M HF. The vial with contents was heated 20 minutes to 95°C and then left overnight at room temperature. Again, no change in the solids amount or appearance could be discerned.

The residual solids were separated from the solution and removed from the hot cell for radiometric examination. The solids were counted by GEA and found to contain 0.531 microcuries (μCi) of <sup>137</sup>Cs but

no other detectible gamma activity. Assuming that the solids weighed 10 milligrams (about half of the residual solids seen for the companion sample SF-12-3), the specific activity was about 50  $\mu\text{Ci }^{137}\text{Cs}$  per gram (g) of sample. As will be seen, the specific activity of the dissolved SF-12-3 fuel sample was about 300  $\mu\text{Ci }^{137}\text{Cs/g}$ , i.e., about 6-times higher than the  $^{137}\text{Cs}$  concentration in the residue.

A particle from the residual solid material was measured by a handheld beta/gamma probe and found to register about 50,000 counts per minute. When tested by an alpha probe, the count rate was about 50 counts per minute. Had the solid speck been undissolved plutonium oxide (assuming 1% detection efficiency and 1 mg solid weight), the alpha count rate would have been about  $10^8$  counts per minute. An estimate of the plutonium concentration in the residual solids can be made based on the ratio of plutonium to  $^{137}\text{Cs}$  for the six analyzed fuel segments (about 0.84  $\mu\text{g Pu}$  per  $\mu\text{Ci }^{137}\text{Cs}$ ; as will be seen in Figure 3.3). If this ratio holds for the undissolved residues, the plutonium concentration would be about 45  $\mu\text{g Pu}$  per gram of residue based on the  $^{137}\text{Cs}$  analysis. As will be seen, sample SF-12-3 contained about 270  $\mu\text{g Pu}$  per gram of dissolved fuel, about 6-times higher than that in the residue.

Though the residual solids from sample SF-12-1 were subjected to extensive leaching contacts, little change in solids quantity was noticed. As seen in Table 3.3, the solids residues represented 0.7% or less of the dissolved fuel weight. The radiometric testing of the leached residues also showed about 6-fold lower specific activity when compared with the specific activity of the dissolved fuel materials themselves. Therefore, the potential contributions of the residual solids to the total fuel (versus cladding) activity was considered to be negligible (i.e., 0.1% or less). No further effort was expended to characterize the residual undissolved solids.

### 3.2.3 Solution Analysis Results

The results of the solution analyses, given in terms of the concentration with respect to the dissolved fuel segment solids and taken from the analytical reports, are provided in Table 3.4. Replicate KPA and AEA data were obtained for sample SF-12-3 and replicate TIMS data obtained for SF-4-2. The replicate SF-12-3 KPA and AEA results were averaged. The replicate for the SF-4-2 uranium and plutonium isotopic TIMS analyses each was run in duplicate in the mass spectrometer. The results from the duplicates were averaged to provide the estimate for the second replicate. The values used in subsequent calculations were obtained by averaging the first and second replicate values. The selected values used in subsequent evaluations are provided under their respective columns in Table 3.4 for samples SF-12-3 (KPA and AEA) and SF-4-2 (TIMS). The results are described in further detail according to the analytical technique in the following sections.

#### *Uranium Concentration by KPA*

Uranium concentrations were determined by KPA. Consistent with the observation of  $\text{UO}_2$  in the XRD analyses of the fuel samples, the uranium concentrations were high in all three fuel items, ranging from 890,000 to 903,000  $\mu\text{g/g}$  of dissolved fuel, or 89.0 to 90.3 wt%. Within the  $\pm 4\%$  KPA relative measurement uncertainty, this number is equivalent to the 88.15 wt% concentration of uranium in stoichiometric  $\text{UO}_2$ .

**Table 3.4. Suspect Fuel Radiochemical Analytical Results As-Reported**

Analysis	SF-4		SF-8		SF-12		Replicates	
	Center	Near End <sup>(a)</sup>	Center	Near End	Center <sup>(b)</sup>	Near End	1 <sup>st</sup>	2 <sup>nd</sup> (Run 1 & 2)
<b>KPA</b>	<b>µg/g Fuel Dissolved</b>							
	<b>SF-4-1</b>	<b>SF-4-2</b>	<b>SF-8-1</b>	<b>SF-8-2</b>	<b>SF-12-3</b>	<b>SF-12-2</b>	<b>SF-12-3</b>	
U	8.99E+05	8.94E+05	8.94E+05	9.03E+05	8.90E+05	8.98E+05	8.92E+05	8.88E+05
<b>TIMS</b>	<b>Atom%</b>							
	<b>SF-4-1</b>	<b>SF-4-2</b>	<b>SF-8-1</b>	<b>SF-8-2</b>	<b>SF-12-3</b>	<b>SF-12-2</b>	<b>SF-4-2</b>	
<sup>233</sup> U	<0.001	<0.001	0.001	<0.001	<0.001	0.001	0.001	<0.001 <0.001
<sup>234</sup> U	0.005	0.005	0.005	0.005	0.003	0.006	0.006	0.003 0.004
<sup>235</sup> U	0.67	0.67	0.67	0.71	0.68	0.71	0.67	0.67 0.67
<sup>236</sup> U	0.009	0.006	0.005	0.003	0.005	0.004	0.007	0.003 0.007
<sup>238</sup> U	99.32	99.32	99.32	99.28	99.31	99.28	99.31	99.33 99.32
<sup>238</sup> Pu, AEA	0.00222	0.00205	0.00160	0.00070	0.00136	0.00104	0.00128 <sup>(c)</sup>	0.00143 <sup>(c)</sup>
<sup>238</sup> Pu	0.011	0.028	0.144	0.360	<0.001	0.019	0.051	0.004 0.005
<sup>239</sup> Pu	97.71	97.93	98.27	98.66	98.58	98.96	98.04	97.80 97.83
<sup>239</sup> Pu, renorm'd. <sup>(d)</sup>	97.72	97.96	98.42	99.02	98.58	98.97	NA	
<sup>240</sup> Pu	2.25	2.03	1.53	0.87	1.41	1.00	1.89	2.19 2.15
<sup>241</sup> Pu	0.021	0.010	0.031	0.06	0.004	0.016	0.013	0.009 0.006
<sup>242</sup> Pu	0.002	0.002	0.020	0.046	0.004	0.009	<0.001	0.003 0.005
<b>AEA</b>	<b>µCi/g Fuel Dissolved</b>							
	<b>SF-4-1</b>	<b>SF-4-2</b>	<b>SF-8-1</b>	<b>SF-8-2</b>	<b>SF-12-3</b>	<b>SF-12-2</b>	<b>SF-12-3</b>	
<sup>237</sup> Np	1.18E-03	1.13E-03	8.71E-04	5.53E-04	7.60E-04	5.20E-04	7.48E-04	7.71E-04
<sup>238</sup> Pu	1.59E-01	1.31E-01	8.01E-02	2.25E-02	6.35E-02	3.29E-02	6.22E-02	6.48E-02
<sup>239,240</sup> Pu	2.76E+01	2.45E+01	1.89E+01	1.20E+01	1.77E+01	1.18E+01	1.83E+01	1.70E+01
<b>GEA</b>	<b>µCi/g Fuel Dissolved</b>							
	<b>SF-4-1</b>	<b>SF-4-2</b>	<b>SF-8-1</b>	<b>SF-8-2</b>	<b>SF-12-3</b>	<b>SF-12-2</b>	NA	
<sup>54</sup> Mn	2.18E-02	2.13E-02	<3.0E-03	6.78E-02	<2.0E-03	<2.0E-03		
<sup>60</sup> Co	1.08E-02	1.13E-02	2.13E-03	3.14E-02	<9.0E-04	<7.0E-04		
<sup>137</sup> Cs	4.95E+02	4.68E+02	3.55E+02	2.21E+02	3.04E+02	2.18E+02		
<sup>154</sup> Eu	5.85E-02	4.69E-02	<5.0E-03	<4.0E-03	<5.0E-03	<3.0E-03		
<sup>239</sup> Pu	<3.0E+02	<2.0E+02	<2.0E+02	<2.0E+02	<2.0E+02	<2.0E+02		
<sup>241</sup> Am	1.00E+00	8.53E-01	3.32E-01	1.01E-01	<2.0E-01	<1.0E-01		

(a) Isotopic results for sample SF-4-2 are averages of the first and second replicate results. The second replicate value is the average of the Run 1 and Run 2 values.

(b) U and <sup>237</sup>Np, <sup>238</sup>Pu, and <sup>239,240</sup>Pu AEA results for sample SF-12-3 are averages of the first and second replicate results.

(c) Based on SF-12-3 values.

(d) The isotopic atom% concentrations for plutonium were renormalized to sum to 100% based on the <sup>238</sup>Pu AEA results. Because of the abundance of <sup>239</sup>Pu, the difference between the as-analyzed and renormalized atom% values are manifest only for this isotope.

### *Uranium and Plutonium Isotopic Analyses by TIMS*

The isotopic compositions of the uranium and plutonium were determined by chemical separation and purification of the uranium and plutonium fractions followed by thermal ionization mass spectrometry, or TIMS. The TIMS analyses showed the uranium to be slightly depleted from the natural concentration of uranium-235 ( $^{235}\text{U}$ ) of 0.7200 atom% (Browne et al. 1986), ranging from 0.67 to 0.71 atom% (at  $\pm 0.01$  atom%). Slight amounts of  $^{236}\text{U}$ , ranging from 0.003 to 0.009 atom% (at  $\pm 0.001$  atom%), give additional evidence for the depletion in  $^{235}\text{U}$  to be caused by irradiation and not because the uranium is from the tails of a uranium isotopic enrichment process.

Uranium irradiation is also consistent with the isotopic concentrations of the associated plutonium. The predominant plutonium isotope is plutonium-239,  $^{239}\text{Pu}$ , with concentrations ranging from about 97.7 to 99.0 atom%. The  $^{240}\text{Pu}$  isotopic concentration ranges from 0.87 to 2.25 atom%.

Isotopic analysis of  $^{238}\text{Pu}$  is complicated by the potential presence of the mass 238 isobar from  $^{238}\text{U}$ . For the suspect fuel samples, in which the  $^{238}\text{U}$  concentration exceeds the  $^{238}\text{Pu}$  concentration by a factor of about  $10^8$ , even trace uranium contamination in the plutonium TIMS analytical preparative sample can overwhelm the  $^{238}\text{Pu}$ . Therefore, the  $^{238}\text{Pu}$  concentration is determined more reliably by AEA. The  $^{238}\text{Pu}$  values as determined by AEA and by TIMS are compared on adjacent lines in Table 3.4. It is seen that even with careful purification, the TIMS analyses for  $^{238}\text{Pu}$  are from  $\sim 5$  to  $\sim 500$ -times higher than those found by AEA.

Because the  $^{238}\text{Pu}$  concentration is determined more reliably by AEA than by TIMS, the AEA results are accepted. The isotopic atom% concentrations were renormalized to sum to 100% based on the  $^{238}\text{Pu}$  AEA results. Because of its abundance, the effect of the renormalization on atom% values is manifest only in the  $^{239}\text{Pu}$ . The renormalized results for  $^{239}\text{Pu}$  are given in Table 3.4 just below the as-analyzed  $^{239}\text{Pu}$  results from TIMS.

### *Alpha Energy Analyses (AEA)*

Plutonium, as  $^{238}\text{Pu}$  and  $^{239,240}\text{Pu}$ , and neptunium, as  $^{237}\text{Np}$ , were determined by anion exchange separation from the starting solution, coprecipitation with neodymium fluoride onto counting disks, and AEA. The energies of the three named analytes are sufficiently different that they can be measured in a single spectral analysis. The energies of  $^{239}\text{Pu}$  and  $^{240}\text{Pu}$  are nearly identical such that only their sum can be measured. Americium-241 is also a significant alpha emitter but its energy is nearly identical to that of  $^{238}\text{Pu}$ . The anion exchange separation technique is sufficient to reject the  $^{241}\text{Am}$  from the plutonium and eliminate  $^{241}\text{Am}$  as an interference in the  $^{238}\text{Pu}$  analysis. The concentrations of  $^{237}\text{Np}$ ,  $^{238}\text{Pu}$ , and  $^{239,240}\text{Pu}$  in units of  $\mu\text{Ci/g}$  dissolved fuel are reported in Table 3.4.

The AEA show that the dominant analyzed source of alpha activity, at about 12-28  $\mu\text{Ci/g}$  of dissolved fuel, is  $^{239,240}\text{Pu}$ . The  $^{238}\text{Pu}$  concentrations range from 0.022 to 0.16  $\mu\text{Ci/g}$ . The  $^{237}\text{Np}$  concentrations range from 0.0005 to 0.001  $\mu\text{Ci/g}$ . In comparison, the  $^{241}\text{Am}$  alpha activity, as derived from the equivalent GEA results, ranges from  $<0.1$  to 1  $\mu\text{Ci/g}$ .

*Gamma Energy Analysis (GEA)*

Samples of each digestion solution were counted directly by gamma detectors for GEA. The predominant radionuclide observed in all samples (Table 3.4) was the fission product, <sup>137</sup>Cs. Fission product europium-154 (<sup>154</sup>Eu) was found in samples from SF-4. Americium-241 (<sup>241</sup>Am) was found in detectable levels for samples taken from SF-4 and SF-8 and was below detection in SF-12. The activation products manganese-54 and cobalt-60 (<sup>54</sup>Mn and <sup>60</sup>Co) were found for both SF-4 and SF-8. Plutonium-239 has a relatively high detection limit by this method and was not found in any sample.

**3.2.4 Mass-Based Concentrations**

Isotopic compositions of uranium and plutonium, expressed as weight percentages, and concentrations of the actinides (uranium, neptunium, plutonium, and americium) in the dissolved fuel on mass bases are provided in Table 3.5 as derived from the analytical data given in Table 3.4. The methods used to determine the mass-based concentrations are described in this section.

**Table 3.5.** Suspect Fuel Radiochemical Analytical Results on Weight Bases

Analysis	SF-4		SF-8		SF-12	
	SF-4-1	SF-4-2	SF-8-1	SF-8-2	SF-12-3	SF-12-2
	Center	Near End	Center	Near End	Center	Near End
<b>TIMS</b>	<b>Mass%</b>					
<sup>233</sup> U	<0.001	<0.001	0.001	<0.001	<0.001	0.001
<sup>234</sup> U	0.005	0.005	0.005	0.005	0.003	0.006
<sup>235</sup> U	0.66	0.66	0.66	0.70	0.67	0.70
<sup>236</sup> U	0.009	0.006	0.005	0.003	0.005	0.004
<sup>238</sup> U	99.32	99.33	99.33	99.29	99.32	99.29
<sup>238</sup> Pu, AEA	0.00221	0.00204	0.00160	0.00069	0.00135	0.00104
<sup>239</sup> Pu	97.72	97.95	98.41	99.02	98.58	98.97
<sup>240</sup> Pu	2.26	2.04	1.54	0.88	1.42	1.00
<sup>241</sup> Pu	0.021	0.010	0.031	0.061	0.004	0.016
<sup>242</sup> Pu	0.002	0.002	0.020	0.047	0.004	0.009
<b>KPA, AEA, GEA, TIMS</b>	<b>µg/g Dissolved Fuel</b>					
U	8.99E+05	8.94E+05	8.94E+05	9.03E+05	8.90E+05	8.98E+05
<sup>237</sup> Np	1.67E+00	1.60E+00	1.24E+00	7.85E-01	1.08E+00	7.38E-01
<sup>238</sup> Pu	9.29E-03	7.65E-03	4.68E-03	1.31E-03	3.71E-03	1.92E-03
<sup>239</sup> Pu	4.10E+02	3.67E+02	2.88E+02	1.87E+02	2.70E+02	1.83E+02
<sup>240</sup> Pu	9.49E+00	7.64E+00	4.51E+00	1.66E+00	3.88E+00	1.86E+00
<sup>241</sup> Pu	9.E-02	4.E-02	9.E-02	1.E-01	1.E-02	3.E-02
<sup>242</sup> Pu	9.E-03	8.E-03	6.E-02	9.E-02	1.E-02	2.E-02
Pu total	4.20E+02	3.75E+02	2.93E+02	1.89E+02	2.74E+02	1.85E+02
<sup>241</sup> Am	2.92E-01	2.49E-01	9.69E-02	2.95E-02	<6.E-2	<3.E-2
<b>KPA, AEA, GEA, TIMS</b>	<b>µg/g Fuel Rod Section</b>					
U	7.67E+05	7.62E+05	7.58E+05	7.39E+05	7.37E+05	7.39E+05
<sup>237</sup> Np	1.43E+00	1.37E+00	1.05E+00	6.42E-01	8.93E-01	6.07E-01
Pu total	3.58E+02	3.19E+02	2.48E+02	1.55E+02	2.27E+02	1.53E+02
<sup>241</sup> Am	2.49E-01	2.12E-01	8.21E-02	2.41E-02	<5.E-2	<3.E-2

*TIMS*

The TIMS results presented in Table 3.4 in terms of atom percentages for the uranium and plutonium isotopes are given on a mass percentage basis in Table 3.5. The mass percentage concentrations were calculated by the following equation as illustrated by the calculation for <sup>235</sup>U in natural uranium:

$$\text{Mass\% isotope} = 100\% \times \frac{\text{Atom\% isotope} \times \text{atomic mass}}{\sum[\text{Atom\% isotope} \times \text{atomic mass}]} =$$

$$100\% \times \frac{0.7200 \times 235.044}{[0.000 \times 233.040 + 0.0055 \times 234.041 + 0.7200 \times 235.044 + 0.000 \times 236.046 + 99.2745 \times 238.051]} = 0.711\%$$

It is seen that the mass percent concentration values are very near the atom percent concentration values.

The renormalized plutonium isotope atom% concentrations based on the <sup>238</sup>Pu AEA values (given in Table 3.4) were used to calculate the plutonium isotope mass% concentrations given in Table 3.5.

*Actinide Element Concentrations*

The mass concentrations for the actinides uranium, neptunium, plutonium, and americium, shown in Table 3.5, are presented based on the dissolved fuel only and based on the total weight of the cut fuel rod section, including fuel, cladding, and undissolved residue. The uranium concentrations in the dissolved fuel, about 90 wt%, were presented in Table 3.4 on a mass basis and discussed in the section describing the KPA findings. Because the cladding comprised about 15 to 18% of the total cut fuel rod mass, the uranium concentrations in the entire fuel rod samples were about 74 to 77 wt%. The plutonium concentrations ranged from about 0.02 to 0.04 wt% of the fuel rod, the neptunium concentrations (all as neptunium-237, <sup>237</sup>Np) were about 0.0001 wt% (or about one part per million), and the americium concentrations as <sup>241</sup>Am were <0.000002 to 0.000008 wt%.

*Actinide Isotope Mass Concentrations*

The mass concentrations of the individual neptunium, plutonium, and americium isotopes are presented in Table 3.5. The <sup>237</sup>Np, <sup>238</sup>Pu, and <sup>241</sup>Am mass concentrations were calculated by dividing their concentrations, expressed as μCi per gram of dissolved fuel, by the specific activities of the individual isotopes (given in Table 3.6).

**Table 3.6.** Isotope Properties (Browne et al. 1986)

Isotope	Half-Life, y	Specific Activity, Ci/g Isotope <sup>(a)</sup>
<sup>237</sup> Np	2.140×10 <sup>6</sup>	7.047×10 <sup>-4</sup>
<sup>238</sup> Pu	8.774×10 <sup>1</sup>	1.712×10 <sup>1</sup>
<sup>239</sup> Pu	2.411×10 <sup>4</sup>	6.202×10 <sup>-2</sup>
<sup>240</sup> Pu	6.563×10 <sup>3</sup>	2.269×10 <sup>-1</sup>
<sup>241</sup> Pu	1.44×10 <sup>1</sup>	1.028×10 <sup>2</sup>
<sup>242</sup> Pu	3.763×10 <sup>5</sup>	3.925×10 <sup>-3</sup>
<sup>241</sup> Am	4.327×10 <sup>2</sup>	3.427×10 <sup>0</sup>

(a) Specific activity calculated from half-life and atomic mass.



The mass concentrations for  $^{239}\text{Pu}$  and  $^{240}\text{Pu}$  were calculated from their combined activities as measured by AEA (in  $\text{Ci } ^{239,240}\text{Pu/g}$  of sample), their individual contributions to their activities, as measured by mass spectrometry, and their specific activities. For example, the isotopic mass concentrations for  $^{239}\text{Pu}$  were calculated using the following formula, as illustrated for sample SF-4-2:

$$\frac{^{239}\text{Pu, g}}{\text{g sample}} = \frac{\text{Ci } ^{239,240}\text{Pu}}{\text{g sample}} \times \frac{\text{TIMS Mass\% } ^{239}\text{Pu}}{\text{TIMS Mass\% } ^{239}\text{Pu} \times \text{Spec. Act. } ^{239}\text{Pu} + \text{TIMS Mass\% } ^{240}\text{Pu} \times \text{Spec. Act. } ^{240}\text{Pu}} =$$

$$\frac{2.45 \times 10^{-5} \text{ Ci } ^{239,240}\text{Pu}}{\text{g}} \times \frac{97.95\%}{97.95 \times 6.202 \times 10^{-2} \text{ Ci } ^{239}\text{Pu/g} + 2.04 \times 2.269 \times 10^{-1} \text{ Ci } ^{240}\text{Pu/g}} = \frac{3.67 \times 10^{-4} \text{ g } ^{239}\text{Pu}}{\text{g sample}}$$

The  $^{240}\text{Pu}$  concentrations were calculated in a similar manner.

The  $^{241}\text{Pu}$  and  $^{242}\text{Pu}$  mass concentrations were calculated based on their mass ratios to  $^{239}\text{Pu}$ , as determined by TIMS, times the respective  $^{239}\text{Pu}$  concentrations. Because the  $^{241}\text{Pu}$  and  $^{242}\text{Pu}$  concentrations were near or at their TIMS detection limits, the mass concentrations are only reported to one significant figure. The calculation is illustrated for the  $^{241}\text{Pu}$  mass concentration in sample SF-4-2:

$$\frac{^{241}\text{Pu, g}}{\text{g sample}} = \frac{^{239}\text{Pu, g}}{\text{g sample}} \times \frac{\text{TIMS Wt\% } ^{241}\text{Pu}}{\text{TIMS Wt\% } ^{239}\text{Pu}} = \frac{3.67 \times 10^{-4} \text{ g } ^{239}\text{Pu}}{\text{g sample}} \times \frac{0.010}{97.95} = \frac{3 \times 10^{-8} \text{ g } ^{241}\text{Pu}}{\text{g sample}}$$

The total plutonium concentrations were calculated as the sums of the individual 238, 239, 240, 241, and 242 isotopes for each sample.

### 3.3 Interpretation of Chemical/Radiochemical Findings

As shown in the preceding discussions, the sample analyses for the SF-4, SF-8, and SF-12 suspect fuel items indicate that these materials are fairly similar to each other. All three fuel rod items contain slightly irradiated  $\text{UO}_2$  fuel, likely originally of natural enrichment, with zirconium cladding. Samples from all three showed similar dissolution behaviors, leaving small quantities of residue that were not soluble in the mixed  $\text{HNO}_3/\text{HCl}$ , HF, or mixed  $\text{HNO}_3/\text{HF}$ .

The composition of the uranium in the  $^{235}\text{U}$  and  $^{236}\text{U}$  isotopes gives evidence that the fuel was initially of natural enrichment. Depletion in  $^{235}\text{U}$  concentration and in-growth of  $^{236}\text{U}$  occur when uranium is exposed to thermal neutron flux as would occur in a reactor. The depletion of  $^{235}\text{U}$  occurs because of fission and because of neutron capture to form  $^{236}\text{U}$ . The thermal neutron fission cross-section for  $^{235}\text{U}$  is 585 barns while the thermal neutron capture cross-section to form  $^{236}\text{U}$  is 99 barns (KAPL 2002). Therefore, the total  $^{235}\text{U}$  depletion cross-section is  $585 + 99 = 684$  barns. The ratio of  $^{235}\text{U}$  depletion to  $^{236}\text{U}$  formation is  $684/99 = 6.9$  for uranium exposed to thermal neutrons. Assuming that the uranium in the suspect fuel was initially of natural enrichment, the  $^{235}\text{U}$  depletion divided by the  $^{236}\text{U}$  production were 5.6, 8.3, 10.0, 3.3, 8.0, and 2.5 for the six analyzed SF-4, SF-8, and SF-12 samples, respectively. The average ratio of  $6.3 \pm 3.0$  is consistent, within analytical error, with the fuel originally being of natural enrichment.

It also was observed for each item that samples taken near the fuel rod centers (SF-4-1, SF-8-1, and SF-12-3) endured more irradiation than the complementary samples taken from the fuel rod ends (SF-4-2, SF-8-2, and SF-12-2, respectively). This is manifest, in each case, by the  $^{137}\text{Cs}$ ,  $^{154}\text{Eu}$ ,  $^{237}\text{Np}$ ,  $^{241}\text{Am}$ , and total plutonium concentrations being higher in the center samples than in the ends while the  $^{239}\text{Pu}$  and (generally)  $^{235}\text{U}$  atom% concentrations are lower. These differences are more pronounced for the SF-8 and SF-12 samples than for the SF-4 samples. The SF-4 fuel apparently underwent more irradiation than the SF-8 and SF-12 samples, whose irradiation exposures seem to be similar given their similar radionuclide concentrations.

Recall that radiological dose readings of each rod (except 13) were made underwater at KW (Ball 2005). The dose rates for each rod ranged from  $2\frac{1}{2}$  to 11 R/hour (versus 1 R/hour background), except those of rods 6 and 7, which were at background. The dose rates were higher at the centers than at the ends (see Table A.1). The observed rod dose rates were significantly lower than were observed for single pass reactor fuel ( $\sim 50$  R/hour) and for N Reactor fuel piece scrap (off-scale at 200 R/hour). The irradiation exposure and radionuclide concentration trends observed in the present characterization testing thus are consistent with the dose rate observations made for the individual suspect fuel rods at KW. An appreciation of the influence of irradiation exposure can be seen in comparing the concentrations of two analytes that were measured with relatively good precision,  $^{137}\text{Cs}$ , the most prominent fission product, and plutonium, the most prominent nuclear breeding product. The correlation is shown in Figure 3.3.

Measurements of fuel diameter, mass per unit length (for the fueled portions without end caps), and cladding thickness, described in Section 2.2.2, may be interpreted in light of knowledge that the cladding is zirconium (likely Zircaloy-2, or Zr-2) and the fuel material is  $\text{UO}_2$ . The dimensional analyses, given in Appendix B, show that the cladding in these lengths of end cap-free fuel rod comprises 15.1 wt% of the fuel segment or, conversely, the  $\text{UO}_2$  fuel is 84.9% of the fuel rod mass. This compares well with results from the fuel digestion which showed, as derived from values in Table 3.1, that the undissolved cladding rings represented  $16.1 \pm 1.5\%$  of the initial fuel disk mass. The dimensional analyses show, in addition, that the density of the  $\text{UO}_2$  within the fuel rods is  $9.83 \text{ g/cm}^3$  or  $\sim 90\%$  of the theoretical density of  $\text{UO}_2$ .

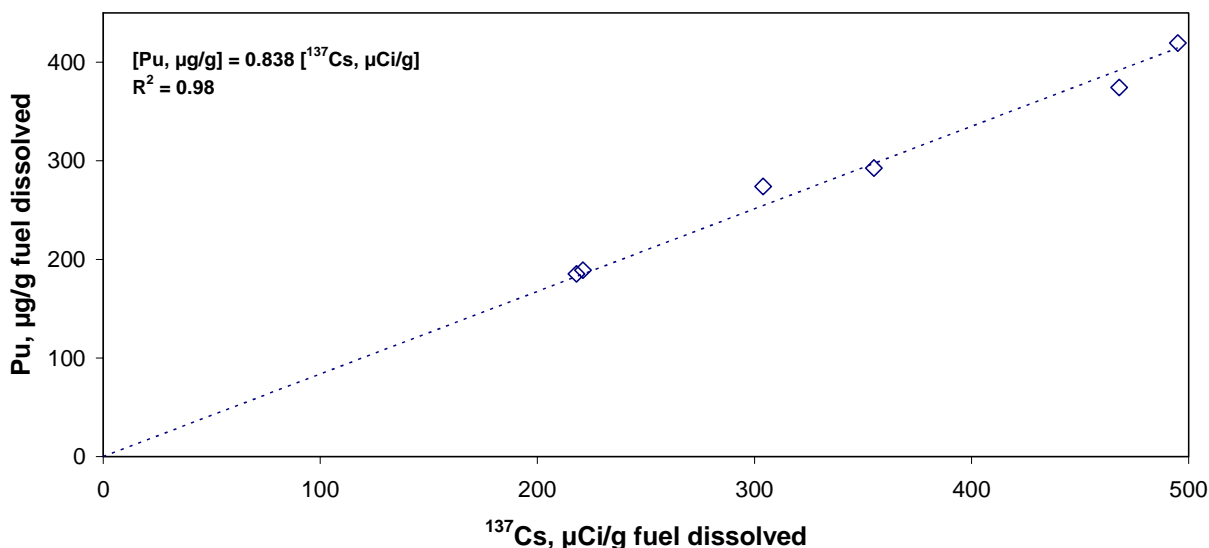


**Figure 3.3.** Correlation of Plutonium Concentration to  $^{137}\text{Cs}$  Concentration in Suspect Fuel Samples

Based on the prior review of Hanford technical literature, it was surmised that the suspect fuel rods were produced during fuel design studies conducted in the late 1950s for the New Production Reactor (NPR; which subsequently became the N Reactor). Among the fuel types being studied were 7-rod clusters which had a single center rod and six rods arranged radially around the center one (Kratzer 1958). These test fuel rods had Zr-2 cladding with 0.56-inch diameter and 0.030-inch thickness and contained natural UO<sub>2</sub> of 85% theoretical density. The SF-4, SF-8, and SF-12 items match, within measurement uncertainty, the Kratzer (1958) items, having zirconium cladding with 0.56-inch diameter and 0.031-inch thickness and containing irradiated natural UO<sub>2</sub> of ~90% theoretical density.

In addition, the test fuel described by Kratzer (1958) has pin-type end caps and wire-wrap (of 0.075-inch diameter) on a 10-inch pitch, similar to the suspect fuel items SF-12 and SF-5 which have pin-type end caps and wire-wrap (estimated ~0.1-inch diameter) with wire wrap markings on the cladding. Fuel item SF-4 has markings suggesting wire wrap on a ~12-inch pitch. Item SF-8 has a flat end cap with v- or y-shaped slots while SF-4 was cut at both ends and thus has no surviving end cap. Reports of test fuel prepared in the late 1950s with slotted flat end-caps, similar to that of SF-8, to accommodate rounded triangular “spider” supports were described in the letter report survey [see footnote (a) in the Introduction section of the present report].

Schwinkendorf (2006) calculated isotope inventories for such fuel based on nominal 0.5-inch fuel rod diameter as found in the present suspect fuel and two <sup>235</sup>U isotopic enrichments, 1.3% and 1.6%, as functions of irradiation exposure. The irradiation conditions chosen were those of the KE Reactor test loop which was used in much of the NPR fuel development testing. The plutonium production and <sup>240</sup>Pu concentrations arising from the 1.3% and 1.6% <sup>235</sup>U enriched fuel as functions of irradiation exposure according to these calculations are summarized in Table 3.7.

**Table 3.7.** Calculated Plutonium Production in Seven-Rod Cluster Prototype Fuel of 1.3 and 1.6 Wt% <sup>235</sup>U Enrichment (taken from Tables 2 and 3, Schwinkendorf 2006)

Parameter, 1.3% <sup>235</sup> U	Exposure, MWD/metric ton U					
	0	778	1621	2556	3581	3860
g Pu/MTU	0	440	890	1330	1750	1860
<sup>240</sup> Pu, %	0	3	6	9	12	12.776
Parameter, 1.6% <sup>235</sup> U	Exposure, MWD/metric ton U					
	0	921	1920	3025	3818	3860
g Pu/MTU	0	450	910	1360	1660	1670
<sup>240</sup> Pu, %	0	3	6	9	11	11.103

The data given in Table 3.7 were regressed to obtain the following equations to calculate the exposure as functions of the plutonium concentration and <sup>240</sup>Pu concentration, respectively, based on the 1.3% <sup>235</sup>U fuel:

- Exposure, MWD/metric ton U = 2.550×10<sup>-4</sup> [Pu, g/10<sup>3</sup> kg U]<sup>2</sup> + 1.598 [Pu, g/10<sup>3</sup> kg U]
- Exposure, MWD/metric ton U = 4.638 [<sup>240</sup>Pu, atom% isotope]<sup>2</sup> + 2.427×10<sup>2</sup> [<sup>240</sup>Pu, atom% isotope]

and 1.6% enriched fuel:

- Exposure, MWD/metric ton U = 2.434×10<sup>-4</sup> [Pu, g/10<sup>3</sup> kg U]<sup>2</sup> + 1.899 [Pu, g/10<sup>3</sup> kg U]
- Exposure, MWD/metric ton U = 5.278 [<sup>240</sup>Pu, atom% isotope]<sup>2</sup> + 2.899×10<sup>2</sup> [<sup>240</sup>Pu, atom% isotope].

As indicated by the slight depletion in <sup>235</sup>U, the presence of <sup>236</sup>U shown in the TIMS results (Table 3.4), and the ratios of the <sup>235</sup>U depletion to <sup>236</sup>U in-growth, the suspect fuel likely was natural uranium, or 0.72 atom% <sup>235</sup>U, before irradiation. Lacking an equation for natural uranium, the results of the present analyses for 1.3% and 1.6% enriched uranium were used to estimate the irradiation exposure (burnup) in the suspect fuel samples. The results, given in Table 3.8, would show lower estimated exposure assuming that the trends observed between 1.6% and 1.3% enrichment continued from 1.3% enrichment down to natural enrichment at 0.72% <sup>235</sup>U. As expected, the exposures estimated for the center samples were greater than those of the corresponding end samples though the differences between the respective SF-4 samples were relatively small. The exposures estimated for the SF-4 samples also were greater than those of the SF-8 or SF-12 samples.

**Table 3.8.** Estimated Irradiation Exposure of Suspect Fuel Samples Based on Correlations for 1.3 and 1.6 Wt% Enriched Fuel Irradiated in the KE Reactor

Analysis Basis	SF-4		SF-8		SF-12	
	SF-4-1	SF-4-2	SF-8-1	SF-8-2	SF-12-3	SF-12-2
	Center	Near End	Center	Near End	Center	Near End
<b>1.3% <sup>235</sup>U</b>	<b>Estimated Exposure, MWD/metric ton U</b>					
g Pu/MTU	802	715	551	346	517	341
<sup>240</sup> Pu, %	570	512	382	215	351	247
<b>1.6% <sup>235</sup>U</b>	<b>Estimated Exposure, MWD/metric ton U</b>					
g Pu/MTU	940	839	648	409	608	402
<sup>240</sup> Pu, %	660	596	450	257	415	295

Because <sup>241</sup>Pu decays to <sup>241</sup>Am with a 14.4-year half-life (meaning 0.04814 of the <sup>241</sup>Pu decays per year), the fuel cooling times can be estimated based on the following equation and the relative <sup>241</sup>Pu and <sup>241</sup>Am concentrations:

$$\text{Cooling time, years} = \frac{-\ln_e \left( \frac{{}^{241}\text{Pu}}{{}^{241}\text{Pu} + {}^{241}\text{Am}} \right)}{0.04814/\text{year}}$$

The results, shown in Table 3.9, are somewhat reproducible for SF-4, which has the most precise <sup>241</sup>Pu and <sup>241</sup>Am measurements, but poor to non-existent for SF-8 and SF-12. The uncertainties in the cooling times are estimated based on the 1-σ errors of the respective <sup>241</sup>Pu and <sup>241</sup>Am measurements.

**Table 3.9.** Estimated Cooling Times Based on Relative <sup>241</sup>Pu and <sup>241</sup>Am Concentrations

Analysis	SF-4		SF-8		SF-12	
	SF-4-1	SF-4-2	SF-8-1	SF-8-2	SF-12-3	SF-12-2
	Center	Near End	Center	Near End	Center	Near End
<sup>241</sup> Pu, μg/g diss. fuel	8.89E-02	3.87E-02	9.17E-02	1.15E-01	1.11E-02	2.99E-02
<sup>241</sup> Am, μg/g diss. fuel	2.92E-01	2.49E-01	9.69E-02	2.95E-02	<6.E-2	<3.E-2
Cooling Time, y <sup>(a)</sup>	30±6	42±14	15±8	5±7	–	–

(a) Cooling time uncertainties based on 1-σ errors in <sup>241</sup>Pu and <sup>241</sup>Am analyses.

For SF-4, the cooling times indicate a discharge date between ~1964 and 1976. The likely discharge dates, if the fuel had been produced during NPR development testing, would be in the late 1950s. The laboratory could provide better estimates of cooling time by extraction and counting measurements for <sup>241</sup>Am, which are more reliable than the reported GEA measurements, and by liquid scintillation counting

of purified plutonium fractions to quantify  $^{241}\text{Pu}$  by its beta decay peak. The present  $^{241}\text{Am}$  measurements suffered high background count rates caused by Compton scattering from high  $^{137}\text{Cs}$  concentrations while the  $^{241}\text{Pu}$  TIMS measurements were near or below the detection limit. Because the accuracy of the present measurements satisfies the original required accuracy objectives given in the SAP for  $^{241}\text{Am}$  and  $^{241}\text{Pu}$ , further analyses of  $^{241}\text{Am}$  and  $^{241}\text{Pu}$  to obtain better estimates of cooling time were not performed.

## 4.0 Quality Assurance and Control Summary

The physical examinations and the laboratory analyses performed on the suspect fuel were conducted in accordance with the SAP (Baker et al. 2006) and the Analytical Support Operations (ASO) Quality Assurance Plan and procedures, which are consistent with the criteria identified in the applicable sections of the OCRWM Quality Assurance Requirements and Description document (DOE 2003).

Table 3.2 summarizes the key analytical QC sample requirements and acceptance criteria specified in the SAP. The SAP QC requirements, including all detection limits, were met for all the analyses, with the exception of a small group of deficiencies (summarized below). Based on the assessment of these deficiencies, through a corrective action review discussed in detail within the Technical Data Package, it was concluded that the deficiencies as resolved did not have a significant impact on overall data quality and further corrective action was unnecessary. All ASO laboratory procedures and QC sample requirements were met.

### *Total Uranium Analyses*

The U-KPA “blank spike” prepared in the hot cell recovered at an un-expectedly high recovery of 263%, which significantly exceeded the  $\pm 20\%$  accuracy criterion identified in the SAP. An investigation was conducted, and it was concluded that the low levels of uranium observed in the “process blank” were an indication that the overall environment in the hot cell was not contaminated with the high levels of uranium that would be needed to account for the high blank spike recovery. The U-KPA instrument calibration and calibration verification show that the instrument was performing within the QC requirements for the method and the SAP (calibration verification achieved was  $\pm 4\%$  vs. SAP criterion of  $\pm 7.5\%$ ). Additional uranium present in the blank spike was most likely the result of the spill of the fuel sample during the sample digestion (see Section 3.2.1). If a similar quantity of additional uranium was present in any of the suspect fuel samples, the effect on measured uranium content would be insignificant (i.e., it would have contributed less than 1% of the measured uranium - within the reported measurement uncertainty of  $\pm 4\%$ ).

The SAP identified a U-KPA matrix spike; however, because the requirement for a “true duplicate” was removed during a revision of the SAP, the requirement for a matrix spike sample by U-KPA should have been also omitted during that SAP revision.

### *Neptunium and Plutonium Analyses*

The SAP specifies that counter instruments will be checked daily with counter control samples to ensure performance is within statistical process control criteria. However, the AEA systems do not have a counter control check standard run (as is done for the gamma spectrum analyses-GEA), but rely on other equivalent measures to ensure data accuracy and quality control. The AEA systems do undergo a primary calibration where the detector efficiencies are determined using NIST-traceable standard sources. Routine calibration verification checks of the alpha counters are not performed due to the concern of potential contamination of the counter.

For the plutonium AEA isotopic analyses,  $^{242}\text{Pu}$  was used as the isotopic tracer in each sample and one matrix spike for the sample batch was prepared. The tracer was added to all samples and the tracer recovery was used to normalize the final results of the other Pu isotopes detected. The use of the isotopic

tracer provides an internal standard with each sample. In the case of this batch Pu isotopic analysis, the tracer recovery ranged from 76% to 106% in the samples. The matrix spike sample prepared with the Pu-AEA had a recovery of 70% (with an associated 28% uncertainty). The quantity of spike added to the sample was small compared to the sample concentration and resulted in higher uncertainty and variability in the matrix spike recovery calculation. The quantity of spike used was determined by evaluation of gross alpha information and a best professional judgment estimate of spike quantity to use was made. Without knowing in advance of the exact amount of Pu present in the sample, the matrix spike sample is susceptible to being outside the optimal level for 100% recovery. [Note: The SAP does not specifically call out a matrix spike for Pu-AEA; however, the SAP includes a footnote stating matrix spike recoveries should be within  $\pm 25\%$ .]

The neptunium AEA analysis does not have the advantage of using an isotopic tracer because alpha-emitting isotopic tracers for neptunium analyses are not available. The sample batch did include a blank spike (81%) and matrix spike (94%) with recoveries within the QC acceptance criteria for the method and SAP.

## 5.0 References

- Baker, RB, DR Duncan, and TL Welsh. 2006. *Sampling and Analysis Plan for Suspect Fuel Pieces Found at the KW Basin (OCRWM)*. KBC-29054, Rev. 0A, Fluor Hanford Inc., Richland, WA.
- Ball, DE. 2005. *Verification Test Report for SPR Fuel, Including Fuel of Unknown Origin (OCRWM)*. SNF-22530, Fluor Hanford Inc., Richland, WA.
- Browne, E, RB Firestone, and VS Shirley. 1986. Table of Radioactive Isotopes, John Wiley and Sons, New York, NY.
- DOE. 2003. *Quality Assurance Requirements and Description*. DOE/RW-0333P, Revision 13, Office of Civilian Radioactive Waste Management, US Department of Energy, Washington DC.
- Fluor. 2006. *One Time Request for Shipment Spent Nuclear Fuel Coupons in the PAS-1 Cask*. HNF-27514, Rev. 0, Fluor Hanford, Richland, WA.
- KAPL. 2002. *Chart of the Nuclides*, 16<sup>th</sup> edition, Knolls Atomic Power Laboratory, Niskayuna, NY.
- Keller, C. 1972. "Lanthanide and Actinide Mixed Oxide Systems with Alkali and Alkaline Earth Metals," chapter 2 in Lanthanides and Actinides, Volume 7 of MTP International Review of Science, *Inorganic Chemistry, Series One*, Butterworths, London, UK.
- Kratzer, WK. 1958. *Production Test IP-213-A, Irradiation of an Eight-Foot UO<sub>2</sub> Seven-Rod Cluster Element*. HW-57865, Hanford Atomic Products Operation, Richland, WA.
- Schwinkendorf, KN. 2006. *Estimation of Isotopic Inventory for Suspect Fuel Piece*. HNF-28302, Rev. 0, Fluor Government Group, Richland, WA.
- Sexton, RA. 2006. *Characterization of Metallic Suspect Fuel Stored in 105 K West (OCRWM)*. HNF-28333, Fluor Hanford, Richland, WA.
- Weakley, EA. 1979. *Fuels Engineering Technical Manual*. UNI-M-61, United Nuclear Industries, Richland, WA.
- Weigel, F. 1986. *Uranium*, page 263, chapter 5 of The Chemistry of the Actinide Elements, 2<sup>nd</sup> edition, JJ Katz, GT Seaborg, and LR Morss, editors, Chapman and Hall, London, UK.



## **Appendix A**

# **Summary of In-Basin Characterization of Suspect Fuel Rod Pieces and Listing of Pieces Identified for Laboratory Analyses**

**Table A.1.** Summary of In-Basin Characterizations of Suspect Fuel Rod Pieces and Listing of Pieces Identified for Laboratory Analyses (from Baker et al. 2006) (All measurements made underwater, before shipment of select fuel rod pieces to PNNL)

Suspect Fuel Rod Piece Number	Length, Inches <sup>(a)</sup>		Measured Fuel Piece Mass (Underwater) <sup>(a)</sup> Pounds	Fuel Type Based on Measured Density <sup>(a)</sup>	RO-7 Probe Reading, <sup>(b)</sup> R/hr	Clad Outside Diameter, In.	Piece to Hot Cells?	
	Piece	Fuel					Ship to 325 Bldg	Analyze or Hold as Contingent
1	20.5	20	1.45	Oxide	5 - 8	0.55	No	NA
2	17.38	17.5	1.20	Oxide	8 - 11	0.55	No	NA
3	18	17.75	1.26	Oxide	3 - 6	0.55	No	NA
<b>4</b>	<b>9.75</b>	<b>9</b>	<b>0.55</b>	<b>Oxide</b>	<b>6 - 7</b>	<b>0.55</b>	<b>Yes</b>	<b>Analyze</b>
<b>5</b>	<b>9.50</b>	<b>9</b>	<b>0.50</b>	<b>Oxide</b>	<b>5.5</b>	<b>0.55</b>	<b>Yes</b>	<b>Hold</b>
6	21.38	NA	0.00	Empty	1	0.60	No	NA
7	6	NA	0.10	Empty	1	0.50	No	NA
<b>8</b>	<b>12.88</b>	<b>12.38</b>	<b>0.90</b>	<b>Oxide</b>	<b>5 - 7</b>	<b>0.55</b>	<b>Yes</b>	<b>Analyze</b>
9	15.5	14.5	0.95	Oxide	5.5 - 7.5	0.55	No	NA
10	17.5	17	1.25	Oxide	4.5 - 5.5	0.55	No	NA
11	6.88	6.38	0.95	Uranium metal	4.5 - 8.5	0.55	No	NA
<b>12</b>	<b>13</b>	<b>12.5</b>	<b>0.95</b>	<b>Oxide</b>	<b>4.5 - 5.5</b>	<b>0.55</b>	<b>Yes</b>	<b>Analyze</b>
13	6	TBD	TBD	Dropped TBD	Not read	0.55	No	NA
14	2.63	NA	0.05	Empty	3.5	0.55	No	NA
15	2.63	NA	0.00	Empty	2.5	0.55	No	NA

Notes: NA = not applicable. TBD = to be determined. Items (in bold) were shipped to RPL for examinations and analysis.  
 (a) Duncan, DR and JP Sloughter. 2005. Internal Memo to AB Carlson (DFSNW) et al., *Characterization of Legacy Fuel [“Suspect Plutonium Recycle Test Reactor (PRTR) Fuel”] to Support Shipment to 325 Building*, 05-KBC/DRD-002 (dated November 22, 2005), Fluor Hanford Inc., Richland, WA. This memo is also provided as Appendix B of the SAP (KBC-29054, Baker et al. 2006).  
 (b) Ball 2005. Background was approximately 1 R/hr. Readings tended to be lower at the ends of the pins and higher in the center.

A.3

## **Appendix B**

### **Sectioning and Labeling Diagrams for Suspect Fuel Pieces, Remnant Piece Summary, and Calculations on Make-Up of Suspect Fuel**

### B.1 Sectioning and Labeling Diagrams

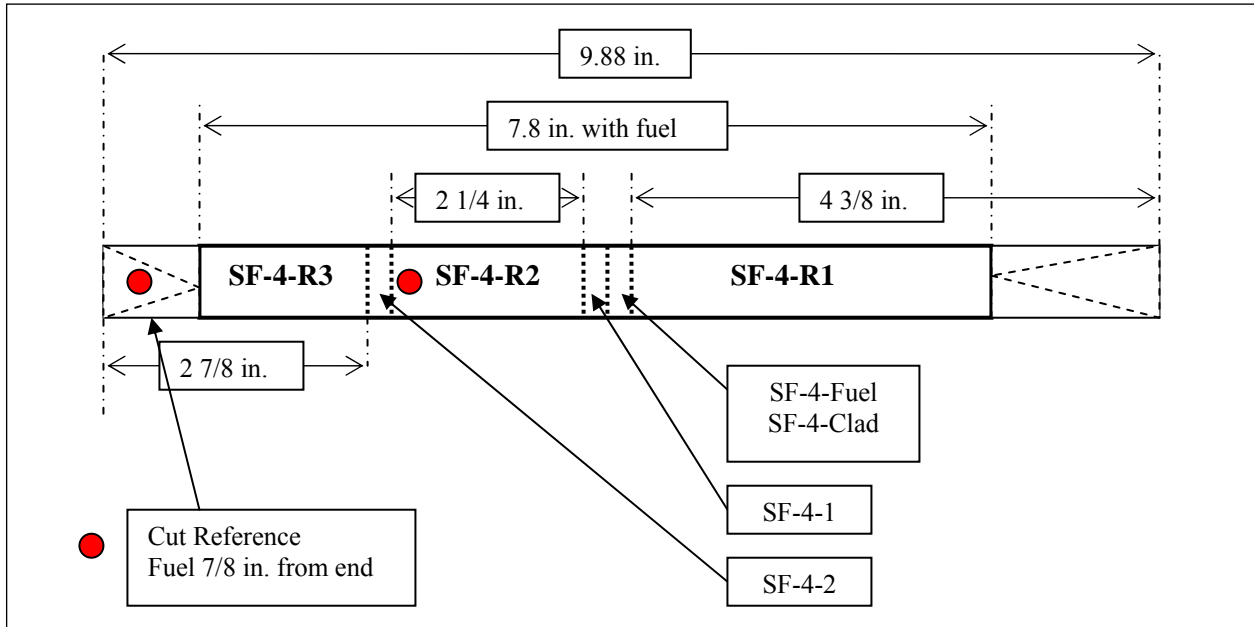


**Figure B.1.** Final Sectioning and Labeling Diagram for Suspect Fuel Rod Piece SF-4  
 (Graphic is simplified – fuel actually extends out each tapered end of rod piece as noted in Section 2.2)

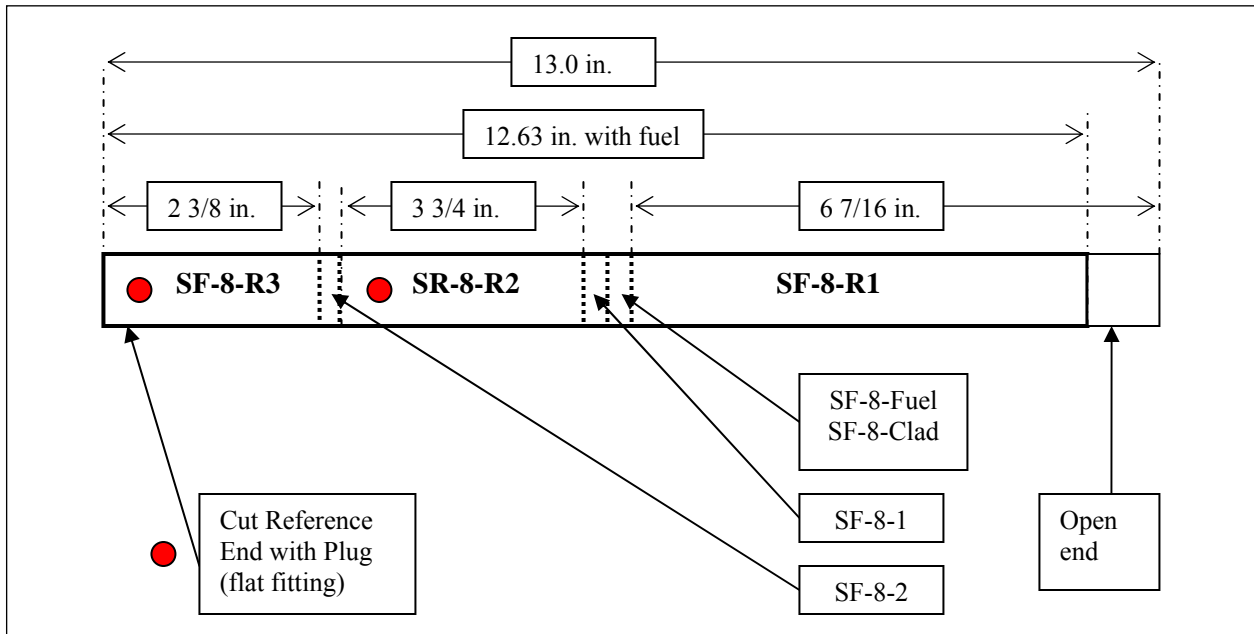


**Figure B.2.** Final Sectioning and Labeling Diagram for Suspect Fuel Rod Piece SF-8  
 [Note: Fueled section was assumed to begin 1/8 inch from reference end.]

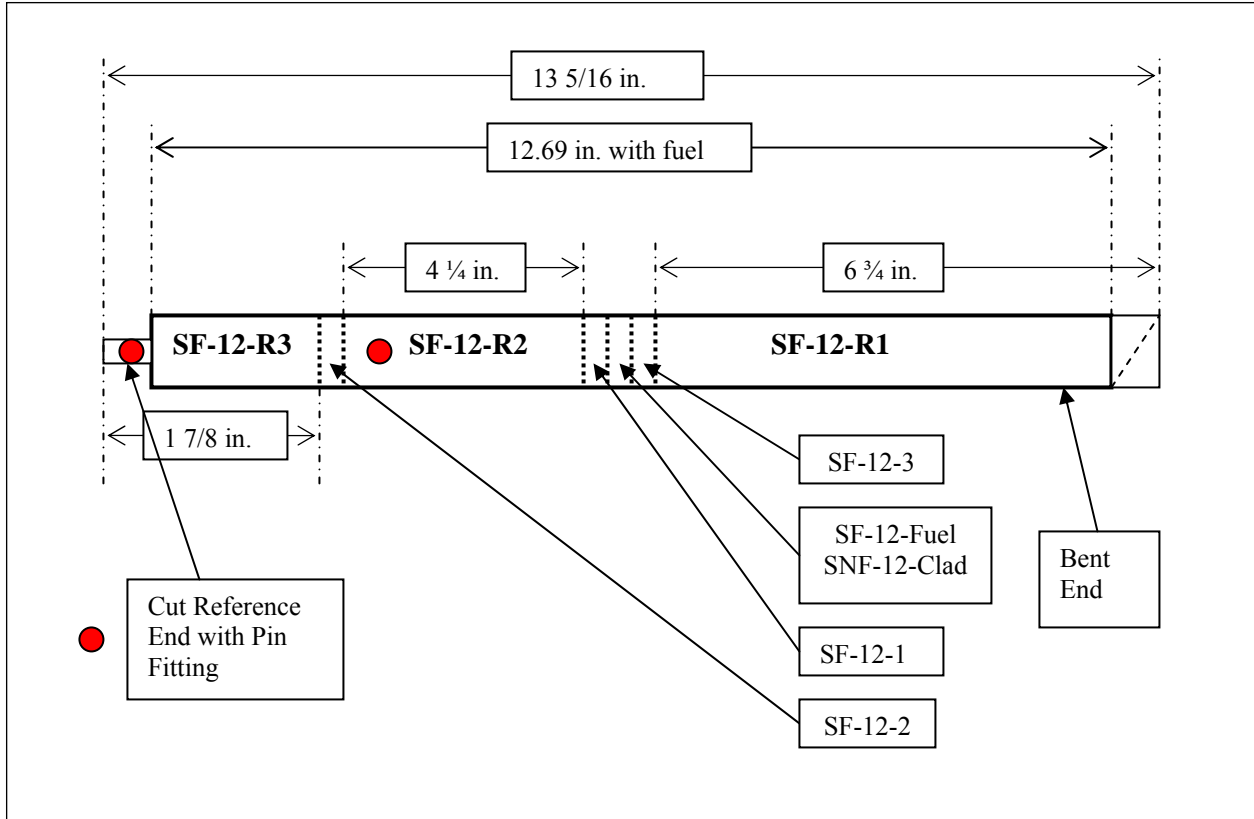


**Figure B.3.** Final Sectioning and Labeling Diagram for Suspect Fuel Rod Piece SF-12  
 [Note: Fueled section was assumed to begin 3/8 inch from fueled end.]

## B.2 Mass and Dimensions of Remnants After Fuel Sectioning

Table B.1 provides information (length and mass) of the remnant pieces created during the section/subsampling of the suspect fuel rod pieces. As shown in Figures B.1 through B.3, remnant pieces labeled “R2” are completely fueled and were used to determine the mass per unit length of fueled rod piece provided in Table 2.2.

**Table B.1.** Mass and Dimensions of Remnants After Suspect Fuel Sectioning

Remnant Piece	Parameter	SF-4	SF-8	SF-12
R1	length, inches	4.38	6.44	6.75
	mass, g	118.8	224.5	232.9
R2	length, inches	2.25	3.75	4.25
	mass, g	82.2	136.4	155.3
R3	length, inches	2.88	2.38	1.88
	mass, g	73.9	66.9	37.3
Scrap <sup>(a)</sup>	mass, g	3.7	3.4	3.8
Remnants Total	mass, g	278.6	431.2	429.3
(a) Primarily, material remaining from sample disk after collecting clad and fuel sample for XRD analysis.				

## B.3 Calculations on Make-Up of Suspect Fuel: Weight Percent Cladding and Fuel Density

The weight fraction of zirconium cladding in the fuel sections and the density of the UO<sub>2</sub> fuel within the measured suspect fuel rods may be calculated based on the data given in Table 2.2 and the density of Zircaloy-2, the likely zirconium metal cladding material. Zircaloy-2 contains ~1.5 wt% tin, ~0.12 wt% iron, ~0.09 wt% chromium, ~0.05 wt% nickel, and the balance zirconium (Weakley 1979).

Thus, the following facts are known about the fuel:

- The average mass per length of the end cap-free fueled rod sections is 36.49 g/inch (from Table 2.2).
- The cladding thickness is 0.031 inch.
- The average outer fuel rod diameter is 0.557 inch (0.55, 0.55, and 0.56 inch for SF-4, SF-8, and SF-12, respectively).
- The theoretical density of UO<sub>2</sub> is 10.95 g/cm<sup>3</sup> (Weigel 1986).
- The density of Zr-2 is 6.55 g/cm<sup>3</sup> (Weakley 1979).

The following statements may be made about the fuel rod by calculation:

- The diameter of the UO<sub>2</sub> cylinders within the fuel is  $0.557 - (2 \times 0.031) = 0.495$  inch.
- The volume of a 1-inch fuel rod segment is  $\pi (0.557/2)^2 \times 1 = 0.244 \text{ in}^3 = 3.933 \text{ cm}^3$ .
- The volume of the UO<sub>2</sub> fuel in a 1-inch segment is  $\pi (0.495/2)^2 \times 1 = 0.192 \text{ in}^3 = 3.15 \text{ cm}^3$ .
- The volume of a 1-inch length of cladding is  $3.93 - 3.15 \text{ cm}^3 = 0.839 \text{ cm}^3$ .
- The mass of cladding in a 1-inch length is  $0.839 \text{ cm}^3 \times 6.55 \text{ g/cm}^3 = 5.50 \text{ g Zr-2}$ .
- The mass of fuel in a 1-inch length is  $36.49 - 5.50 = 30.99 \text{ g}$ .
- The fuel rod is  $100 \times 5.50 / 36.49 = 15.1 \text{ wt\% cladding}$ . This may be compared with, and is consistent with,  $16.1 \pm 1.5 \text{ wt\%}$  as measured for fuel rod disks based on the data in Table 3.1.
- The density of the UO<sub>2</sub> in the fuel is  $30.99 \text{ g} / 3.15 \text{ cm}^3 = 9.83 \text{ g/cm}^3$ .
- The UO<sub>2</sub> fuel density is  $100 \times 9.83 / 10.95 = \sim 90\%$  of theoretical UO<sub>2</sub> density.